Institute of Optical Materials and Technologies
"Acad. Jordan Malinowski" – Bulgarian Academy of Sciences

University of Chemical Technology and Metallurgy – Sofia, Bulgaria

Polarization holography:

Principles, Materials and Applications

Lian Nedelchev

OPTICA Webinar, 29th March 2023

Bulgarian Academy of Sciences (BAS)

- BAS was established more than 150 years ago, in **1869**
- It includes 42 **Institutes** and 8 **Laboratories** and about **3000** scientists
- BAS produces about half of the scientific output of the country
- The H-index of BAS is 211, the H-index of Bulgaria is 280 (2020)

Institute of Optical Materials and Technologies with Bulgarian Academy of Sciences (IOMT – BAS)

- IOMT was established in 2010, by the merger of two Laboratories, found in 1970s
- Staff: about 50 researchers and PhD students
- Annual research activity: about 100 papers in peer-reviewed journals
- Numerous projects with national, EU and international funding

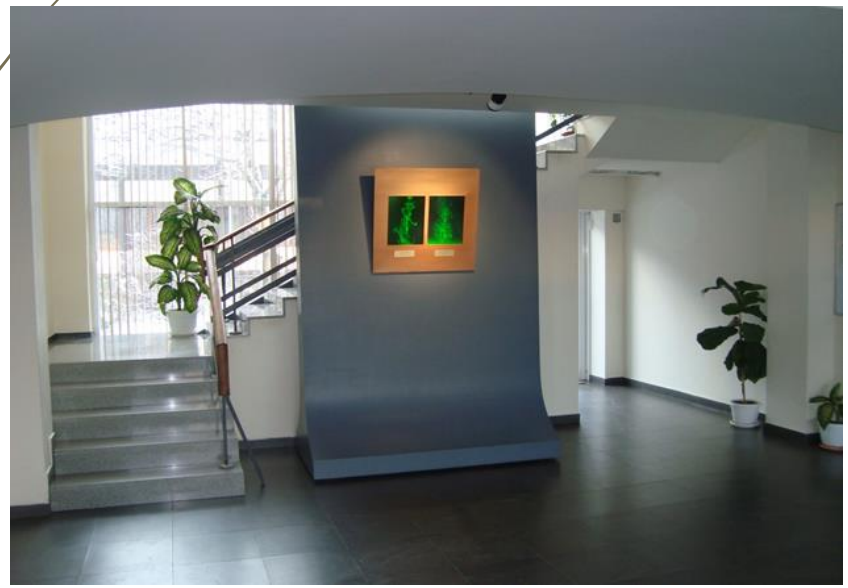

https://iomt.bas.bg/

University of Chemical Technology and Metallurgy (UCTM)

- Since the beginning of 2023, our group started close collaboration with UCTM within a project BiOrgaMCT (Photoanisotropic materials for polarization holography and photonics applications) funded by **NextGenerationEU**
- UCTM is found in 1953 and now has over 2000 students in Bachelor, Master and PhD programs.

https://uctm.edu/en/

Outline

- **From Holography to Polarization holography:**
  General principles and concepts
- **Materials for polarization holography:**
  Types, characterization and main parameters
- **Important applications:**
  Polarization-selective diffractive optical elements, surface relief gratings, digital polarization holography

From Holography to Polarization holography:
General principles and concepts

Holography

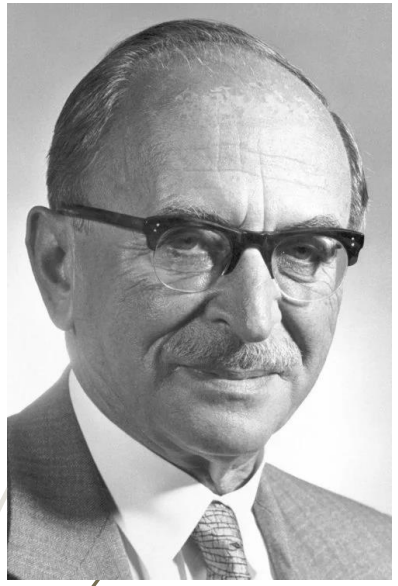

Dennis Gabor
1947 – Invention of the holographic method
1971 – Nobel prize in Physics

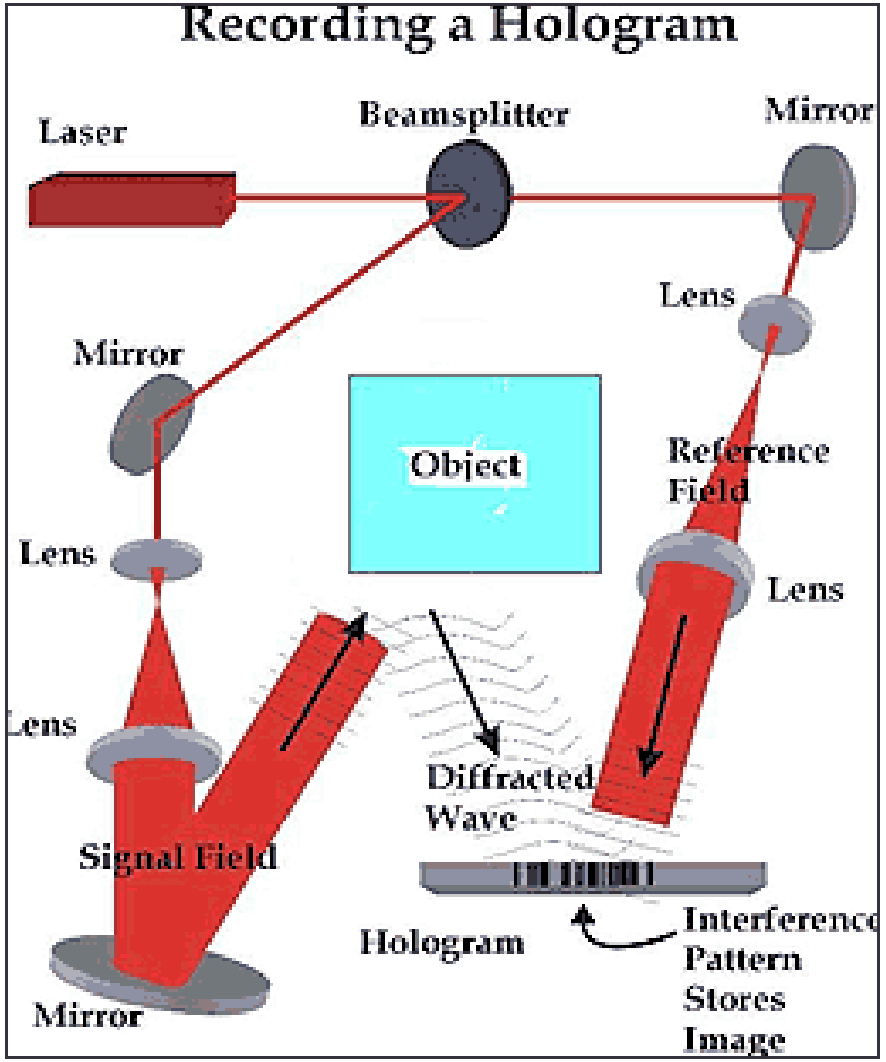

Holography allows to register not only the **intensity**, but also the **phase** of light (3D effect, parallax).

Are these **all** parameters of the light waves…?

1960 – Invention of the laser
1962 – First optical holograms: Emmett Leith and Juris Upatnieks (USA), Urii Denisyuk (USSR)

Polarization holography? Just a theoretical idea?

GENERALIZED THEORY OF INTERFERENCE, AND ITS APPLICATIONS

Part I. Coherent Pencils

BY S. PANCHARATNAM

(*Memoir No. 88 of the Raman Research Institute, Bangalore-6*)

Received October 30, 1956

Reconstruction of Vectorial Wavefronts

A. W. Lohmann

IBM Systems Development Division, Development Laboratory, San Jose, California.
Received 24 May 1965.

Wavefront reconstruction[1] has been aptly termed *holography* which can be translated as *total recording*. The term *total* is used because both the amplitude and the phase of the light wave are recorded, whereas in normal photography, one records only the amplitude. However, at the present time a hologram is not really a total recording, since only one amplitude and one phase are recorded, which would be adequate if light were a scalar wave. The electrical field in the hologram plane contains two vector or polarization components, both with amplitude and phase. We

Kakichashvili, Opt. Spectrosc. **33**, 324 (1972)

Polarization of light

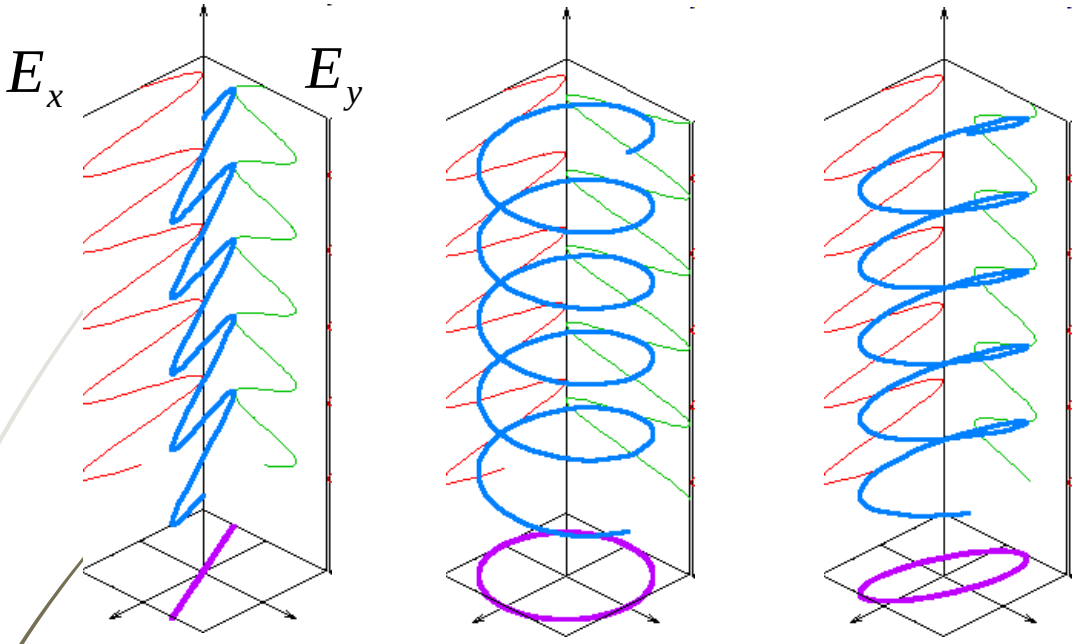

linear **circular** **elliptical**

Poincaré sphere

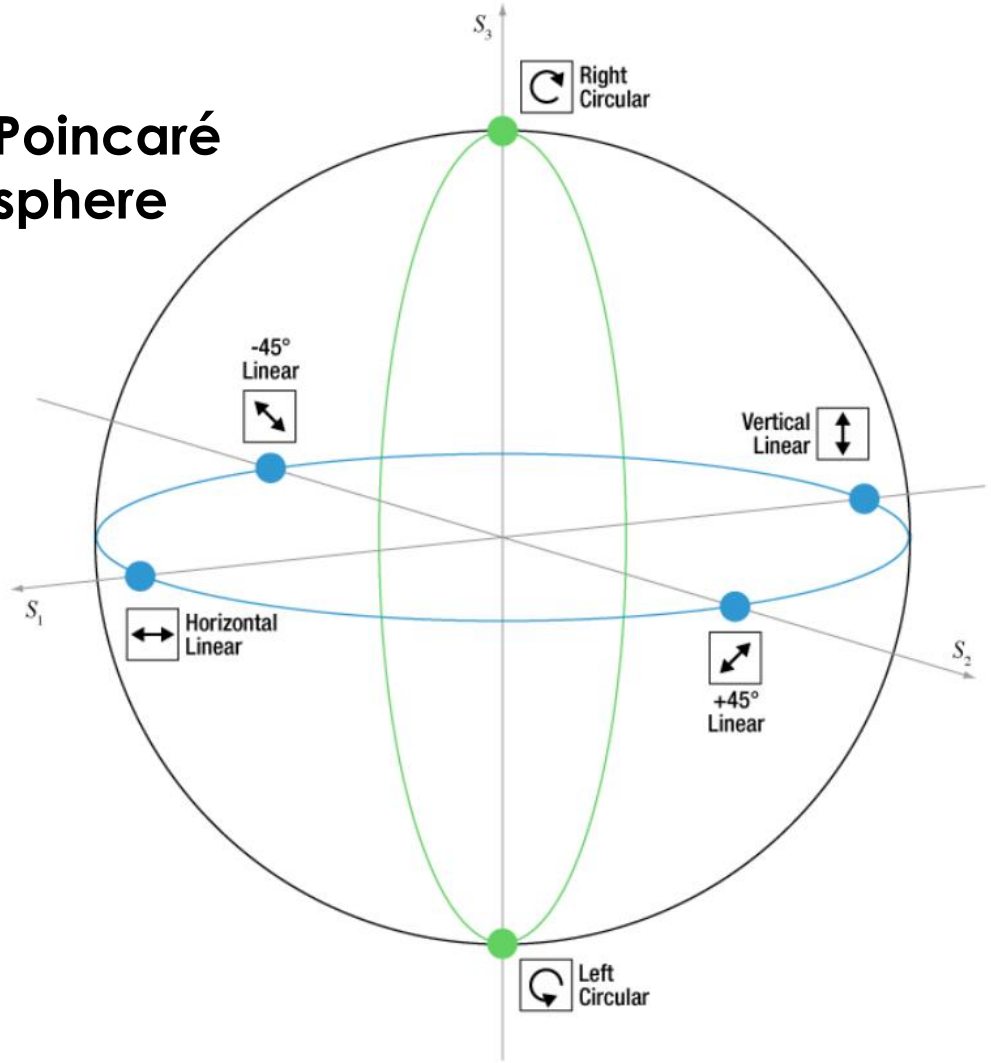

3D cinema glasses

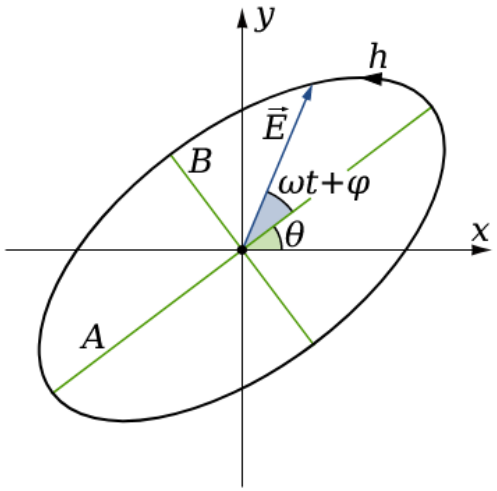

azimuth – ***θ***
ellipticity angle – ***ε***
ellipticity – ***e = tan(ε)***
handedness – ***h*** (left/right)

Stokes vector: $S = \begin{bmatrix} S_0 \\ S_1 \\ S_2 \\ S_3 \end{bmatrix}$

Jones vectors and matrix formalism

The **amplitude** and **phase** information can be conveniently represented as a two-dimensional complex vector (the **Jones vector**). Introduced in 1941 by R. C. Jones, it is applicable for **completely** polarized light.

$$\vec{E} = \begin{pmatrix} E_{0x} e^{i\phi_x} \\ E_{0y} e^{i\phi_y} \end{pmatrix}$$

Normalized Jones vectors for common polarization states:

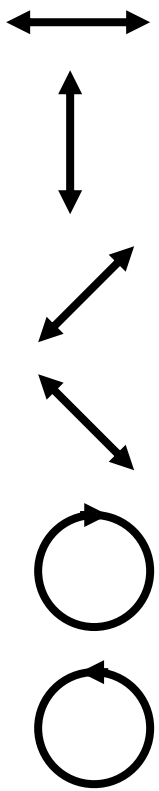

$$\begin{pmatrix} 1 \\ 0 \end{pmatrix}$$

$$\begin{pmatrix} 0 \\ 1 \end{pmatrix}$$

$$\frac{1}{\sqrt{2}}\begin{pmatrix} 1 \\ 1 \end{pmatrix}$$

$$\frac{1}{\sqrt{2}}\begin{pmatrix} 1 \\ -1 \end{pmatrix}$$

$$\frac{1}{\sqrt{2}}\begin{pmatrix} 1 \\ -i \end{pmatrix}$$

$$\frac{1}{\sqrt{2}}\begin{pmatrix} 1 \\ i \end{pmatrix}$$

Every polarizing optical element can be represented by a 2x2 ***Jones matrix* T**, which transforms the Jones vector by a matrix multiplication.

$$E_{out} = \mathbf{T} E_{in}$$

$$E_{out} = \mathbf{T_N} \ldots \mathbf{T_2} \mathbf{T_1} E_{in}$$

Jones matrices for a linear polarizer and retardation plates:

Horizontal linear polarizer: $\mathbf{T} = \begin{bmatrix} 1 & 0 \\ 0 & 0 \end{bmatrix}$

Half-wave plate (HWP): $\mathbf{T_{HWP}} = \begin{bmatrix} 1 & 0 \\ 0 & -1 \end{bmatrix}$

Quarter-wave plate (QWP): $\mathbf{T_{QWP}} = \begin{bmatrix} 1 & 0 \\ 0 & i \end{bmatrix}$

R. C. Jones, J. Opt. Soc. Am. **31**, 488 (1941)

Jones matrices

Jones matrix of a **birefringent media:**

$$\mathbf{T} = \begin{bmatrix} \exp(-i\varphi_1) & 0 \\ 0 & \exp(-i\varphi_2) \end{bmatrix}, \quad \varphi_1 = \frac{2\pi d}{\lambda} n_1, \varphi_2 = \frac{2\pi d}{\lambda} n_2,$$ which can be simplified to:

$$\mathbf{T} = \begin{bmatrix} 1 & 0 \\ 0 & \exp(i\Delta\varphi) \end{bmatrix},$$ where $$\Delta\varphi = \frac{2\pi d}{\lambda}\Delta n, \qquad \Delta n = n_2 - n_1$$ is the **birefringence**.

Jones matrix of an **optically active media:**

$$\mathbf{T} = \begin{bmatrix} \cos(\alpha d) & \sin(\alpha d) \\ -\sin(\alpha d) & \cos(\alpha d) \end{bmatrix},$$

where *d* is the thickness of the material, *α* is the **angle of rotation per unit length**.

Jones matrices can also be calculated for a **polarization grating**.
In this case however, the matrix elements have periodic spatial dependence, corresponding to the positions of the diffracted orders.

Azzam, Bashara. Ellipsometry and polarized light (1977)
Nikolova, Ramanujam. Polarization holography (2009)

Stokes vectors and Mueller matrix formalism

Stokes vector: $S = \begin{bmatrix} S_0 \\ S_1 \\ S_2 \\ S_3 \end{bmatrix}$

$$S_0 = \langle E_x^2(t) \rangle + \langle E_y^2(t) \rangle = I_x + I_y$$

$$S_1 = \langle E_x^2(t) \rangle - \langle E_y^2(t) \rangle = I_x - I_y$$

$$S_2 = 2\langle E_x(t) Ey(t) \cos[\varphi_y - \varphi_x] \rangle = I_{+45°} - I_{-45°}$$

$$S_3 = 2\langle E_x(t) Ey(t) \sin[\varphi_y - \varphi_x] \rangle = I_R - IL$$

$$S_{out} = \boldsymbol{M} S_{in}$$

$$DOP = \frac{\sqrt{S_1^2 + S_2^2 + S_3^2}}{S_0}$$ - degree of polarization (DOP)

$$\theta = \frac{1}{2} \arctan\left(\frac{S_2}{S_1}\right)$$ - azimuth

$$\varepsilon = \frac{1}{2} \arcsin\left(\frac{S_3}{\sqrt{S_1{}^2 + S_2{}^2 + S_3{}^2}}\right)$$ - ellipticity angle

M is a 4 x 4 **Mueller matrix** with real elements, representing the polarization properties of the optical element/sample/system.

Note: Stokes/Mueller formalism allows to describe **partially polarized** light and depolarizing optical systems. However, it operates on intensities and **cannot describe interference or diffraction effects**.

Interference of waves with orthogonal polarizations

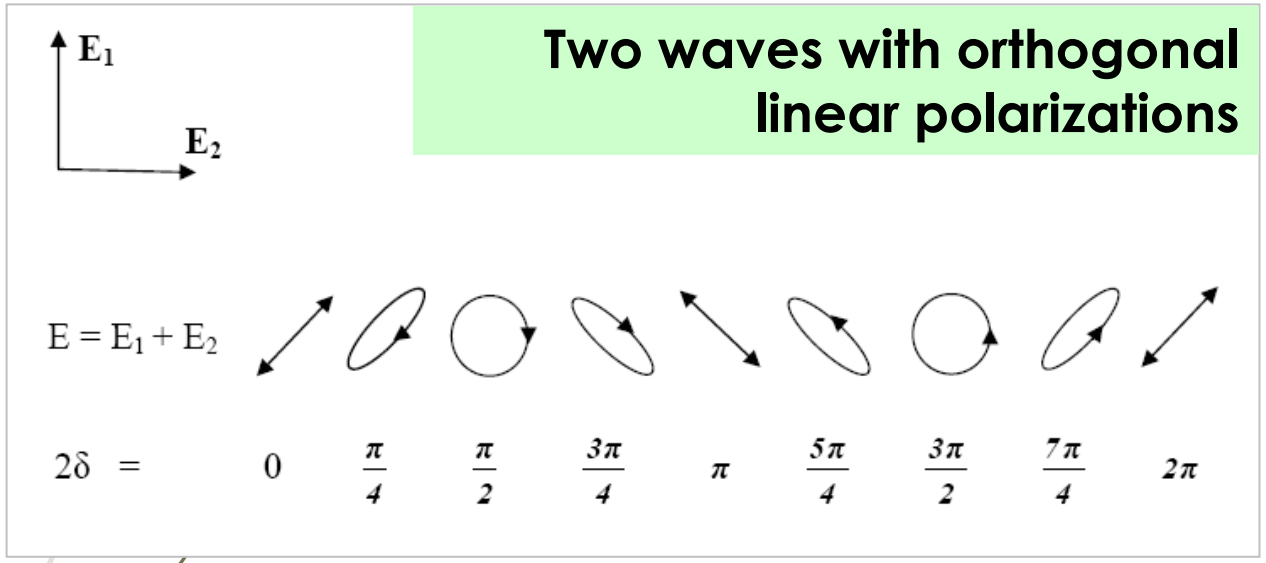

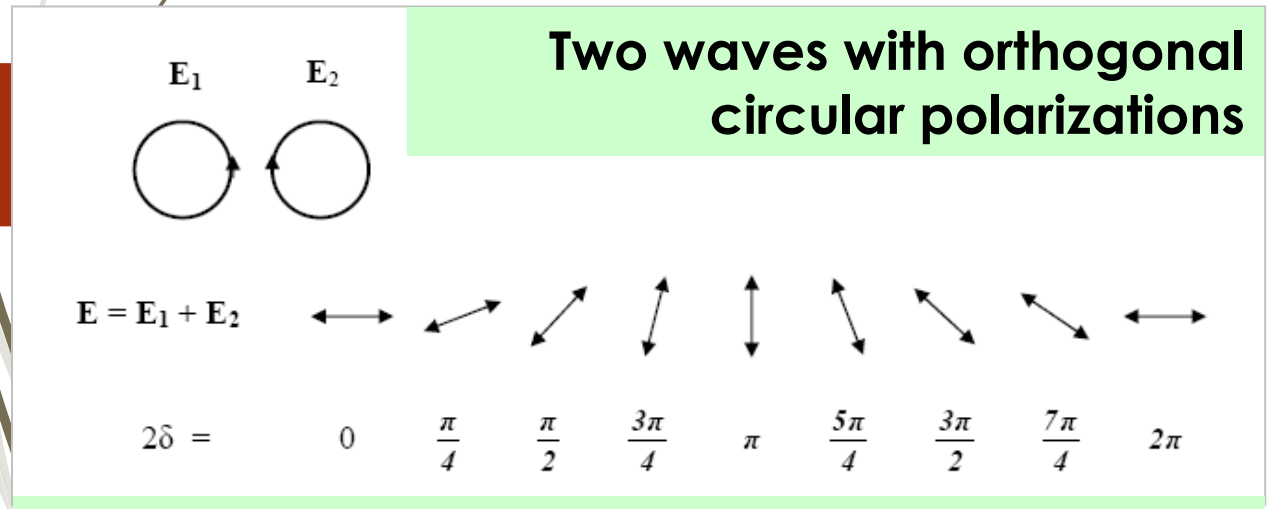

***δ* – phase difference**

In both cases:

- Intensity is **constant**;
- Only the **polarization** is modulated;

Question:
How can we record a polarization hologram in intensity-only-sensitive media?

Answer: …
We need a polarization-sensitive material, or in other words – a **photoanisotropic material**!

Polarization holography: optical schemes

Polarizing beam splitter (PBS)

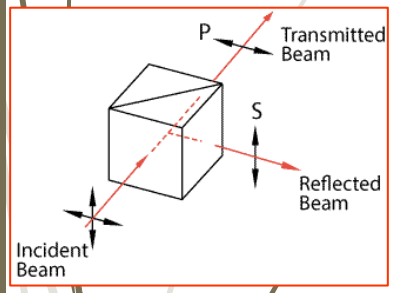

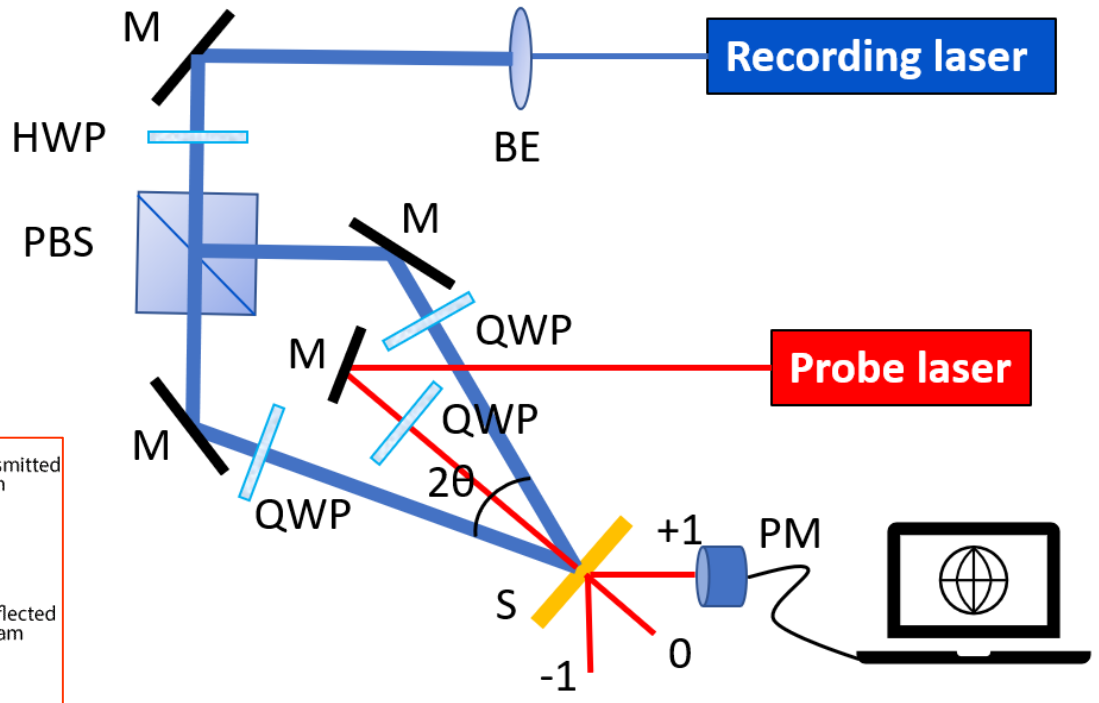

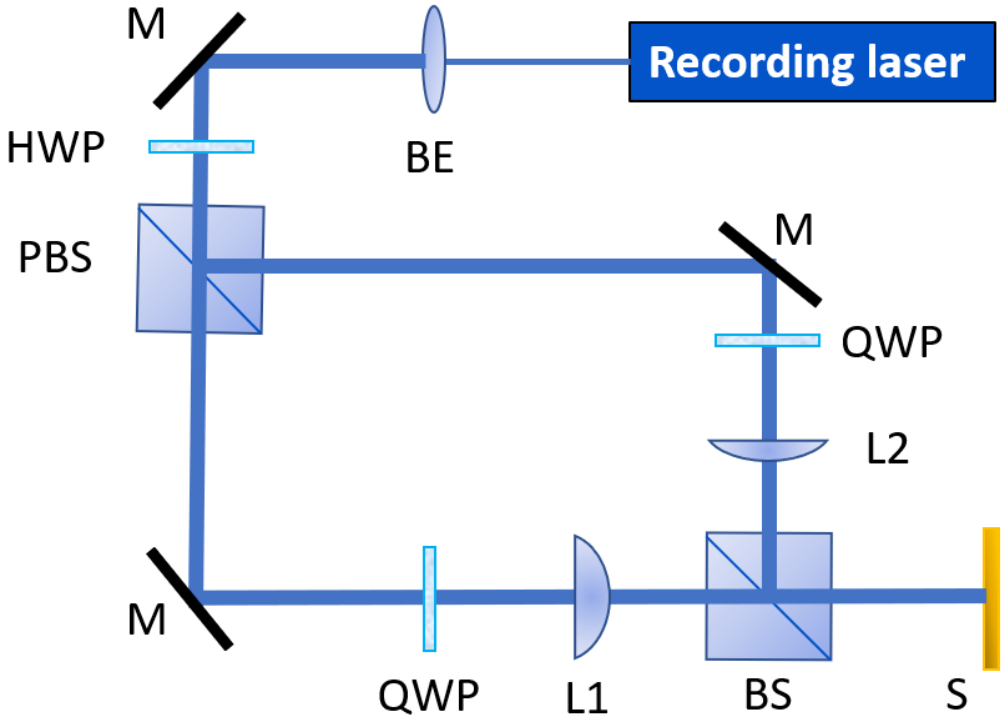

$$\Lambda = \frac{\lambda_{rec}}{2\sin\theta}$$ - period of the grating

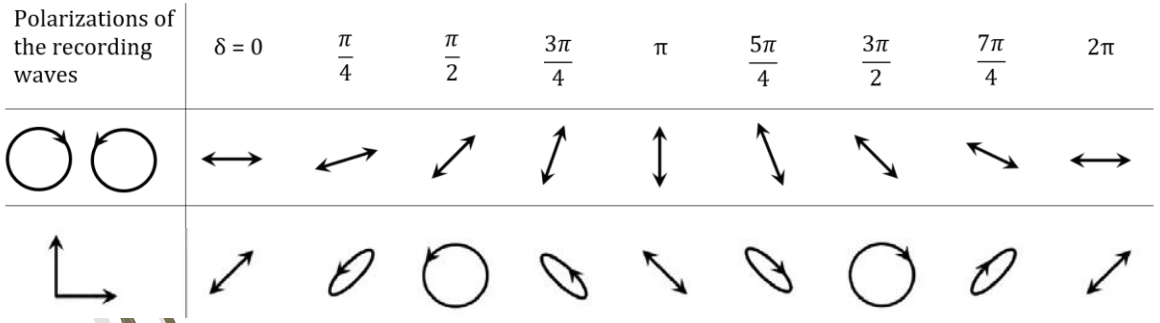

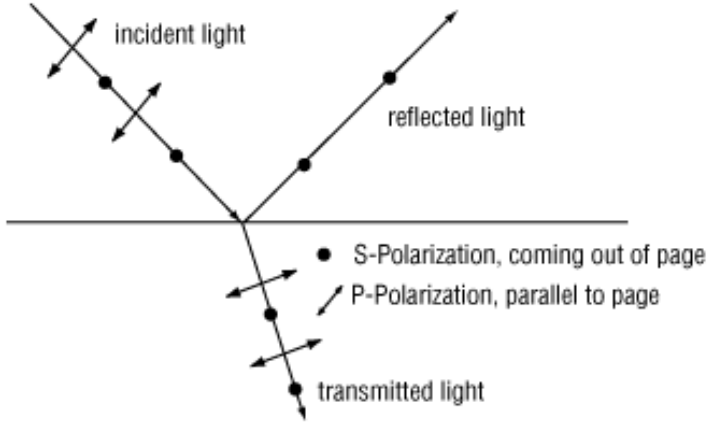

p-polarization: **parallel** to the plane of incidence

s-polarization: **normal** to the plane of incidence

Materials for polarization holography:

Types, characterization and main parameters

Weigert effect

1919

First observation of photoinduced anisotropy!

<u>Definition</u>: Dichroism induced in a silver-silver halide photographic emulsion by a beam of linearly polarized light.

Studies in 1970s revealed that it is due to chains of Ag nanospheres oriented either parallel or perpendicular to polarization of light.

Polarization holographic gratings recorded in AgCl emulsions using the Weigert effect:

- Limitations: low diffraction efficiency (<4%)
- Advantages: high stability (more than 10 years)

Weigert, Verh. Deutsch. Phys. Ges. **21**, 479 (1919)
Nikolova et al, J. Mod. Opt. **39**, 1953 (1992)

High-efficiency photoanisotropic material

1984

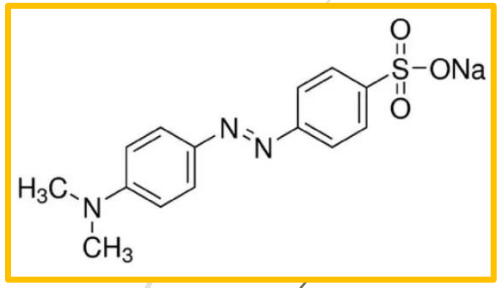

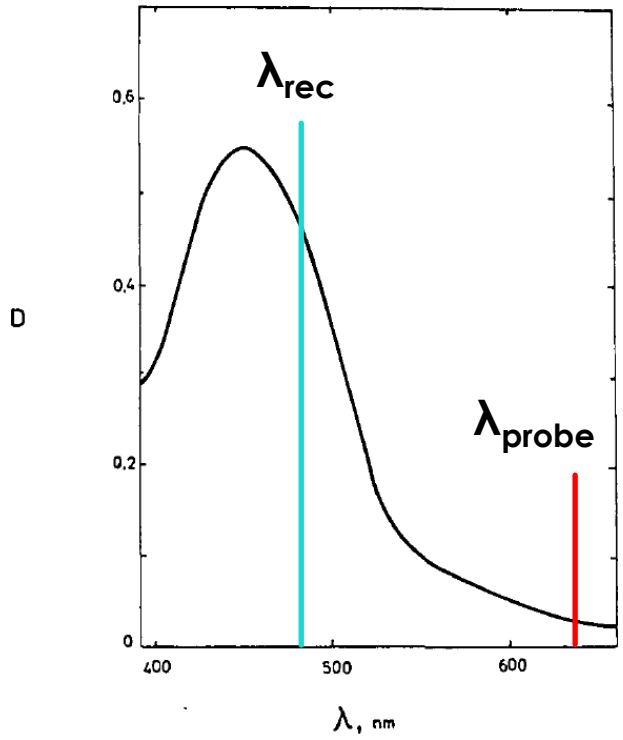

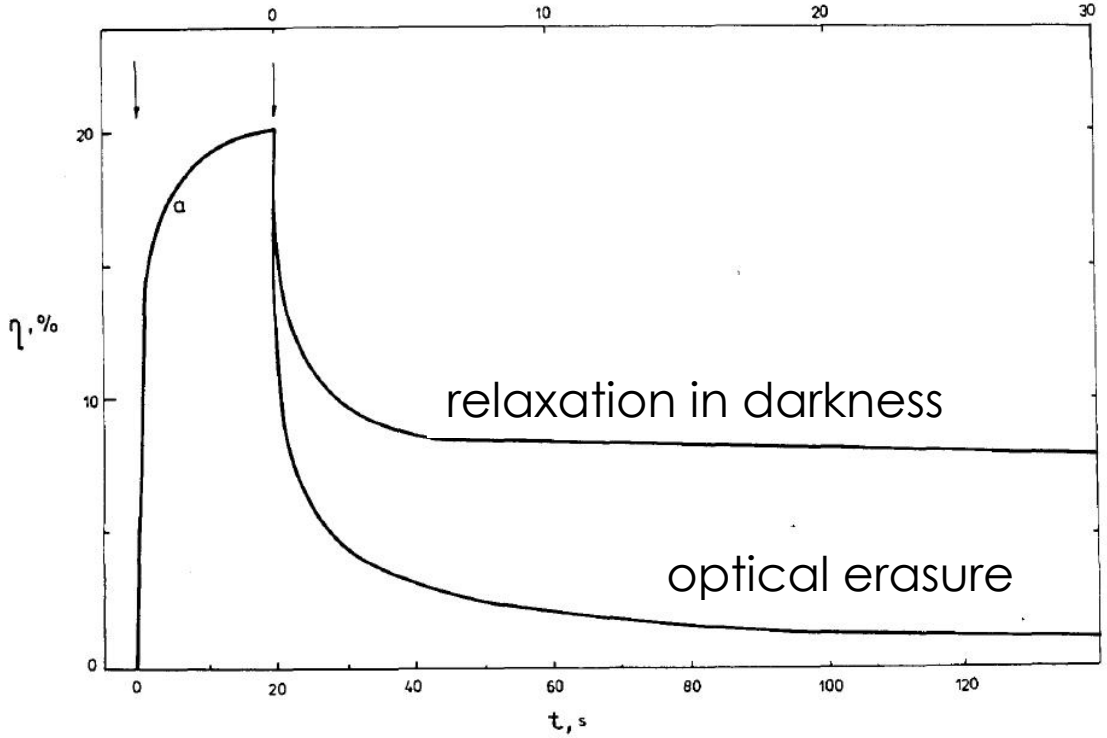

- **Azo dye Methyl Orange** in Poly(vinyl alcohol)
- Film thickness ≈ 100 μm, dye conc. = 0.06 wt. %
- λ_{rec} = 488 nm (Ar+), λ_{probe} = 633 nm (He-Ne)
- Photoinduced birefringence: $\boldsymbol{\Delta n > 10^{-3}}$
- Diffraction efficiency: $\boldsymbol{\eta > 35\%}$

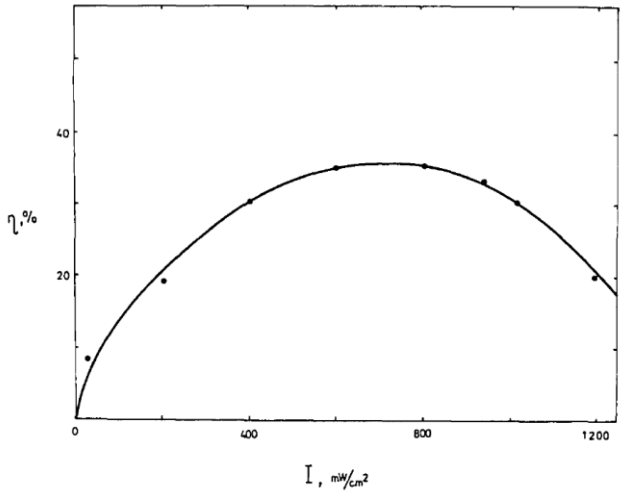

Todorov *et al*, Appl. Opt. **23**, 4309 (1984)

Mechanism of polarization recording in azobenzenes

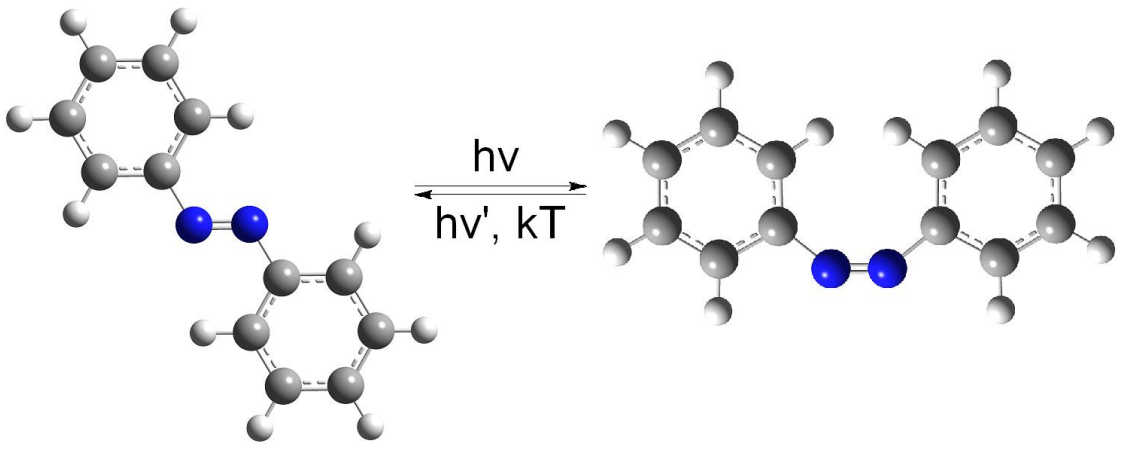

trans
(anisotropic)

cis
(isotropic)

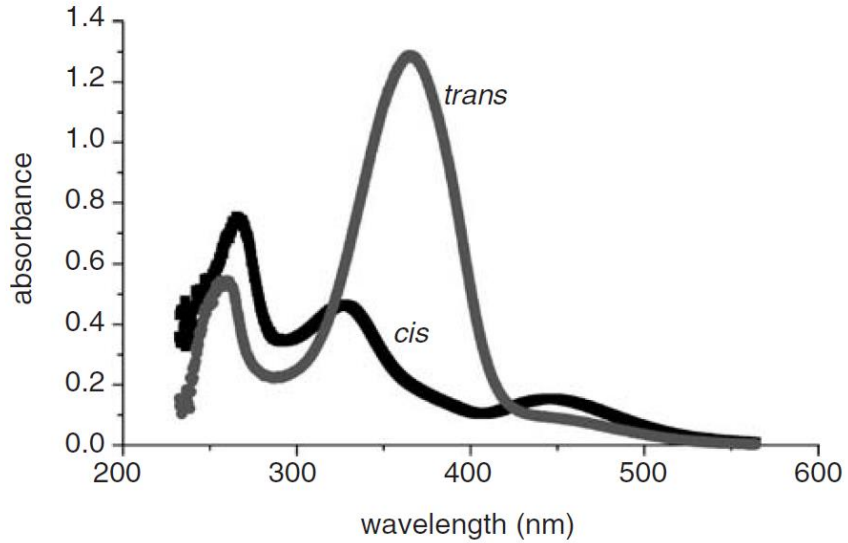

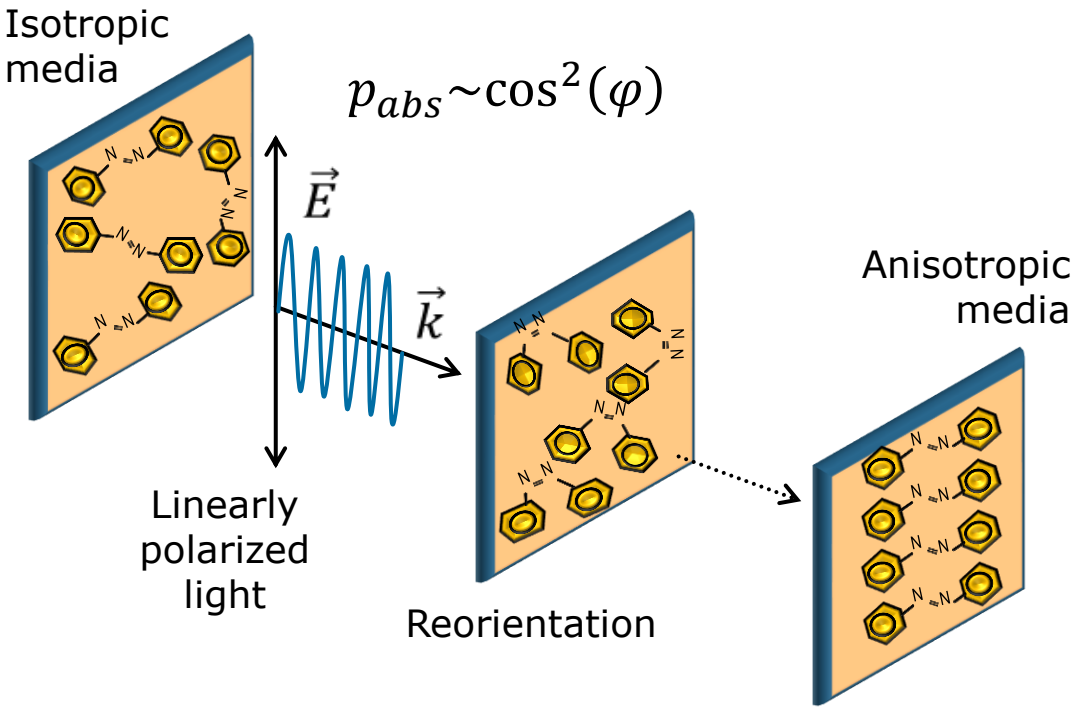

Azochromophores undergo series of *trans-cis-trans* isomerizations until they **reorient perpendicularly** to the electric vector of light.

In this way the polarization of light is recorded in the form of **photoinduced anisotropy** (more often **birefringence**).

Hartley, Nature **140**, 281 (1937)
Pedersen et al, J. Opt. Soc. Am. B **15**, 2721 (1998)

Azodye systems

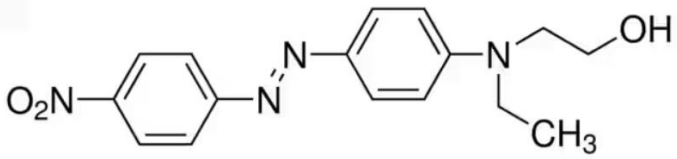

Disperse Red 1 | CAS 2872-52-8

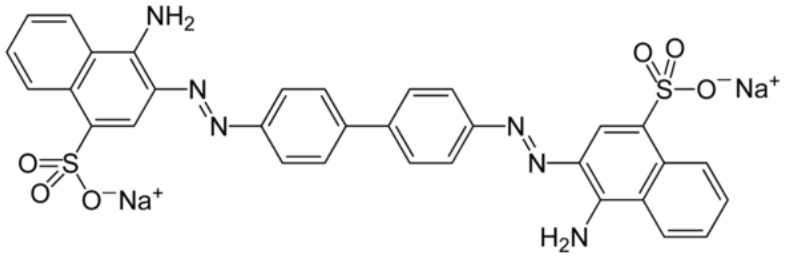

Congo Red | CAS 573-58-0

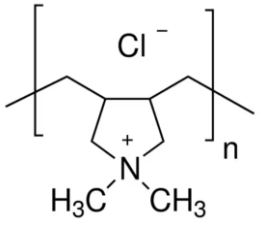

PDAC | CAS 26062-79-3

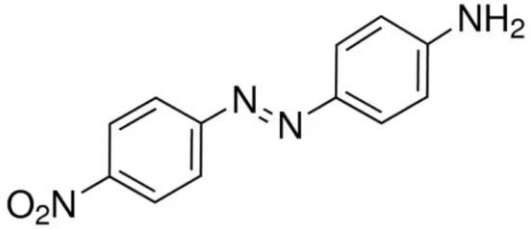

Disperse Orange 3
CAS 730-40-5

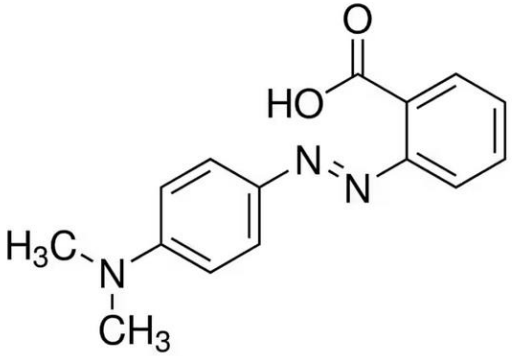

Methyl Red | CAS 493-52-7

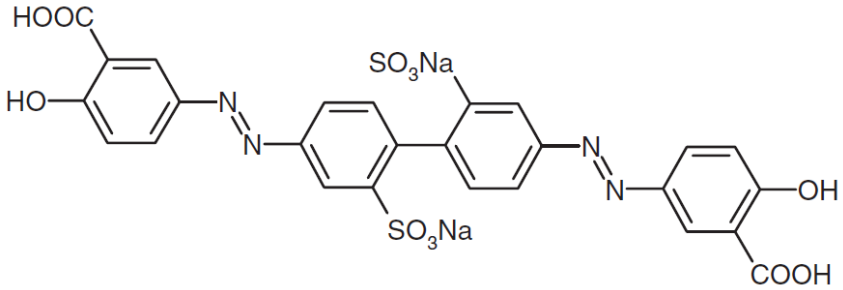

Sulfuric azodye SD-1

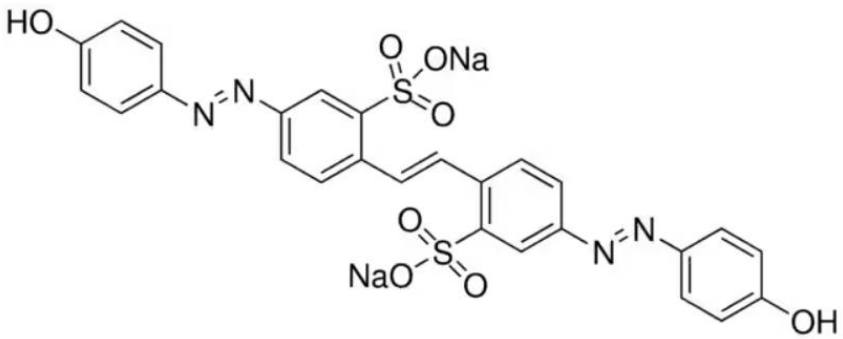

Brilliant Yellow | CAS 3051-11-4

Bian et al, Adv. Mater. **12**, 1202 (2000) – CR/PDAC
Tawa et al, Polymer **41**, 3235 (2000) – DO3
Zhang et al, Opt. Lett **27**, 1105 (2002) – DR1
Yaroshchuk et al, Jap. J. Appl. Phys. **46**, 2995 (2007) – SD1
Yin et al, Opt. Expr. 27, 5814 (2019) – BY
Ahmad et al, Polym. Bull. **78**, 1189 (2021) – MR

From azodyes to azopolymers

1987

The azochromophore is **chemically attached** to the polymer chain.

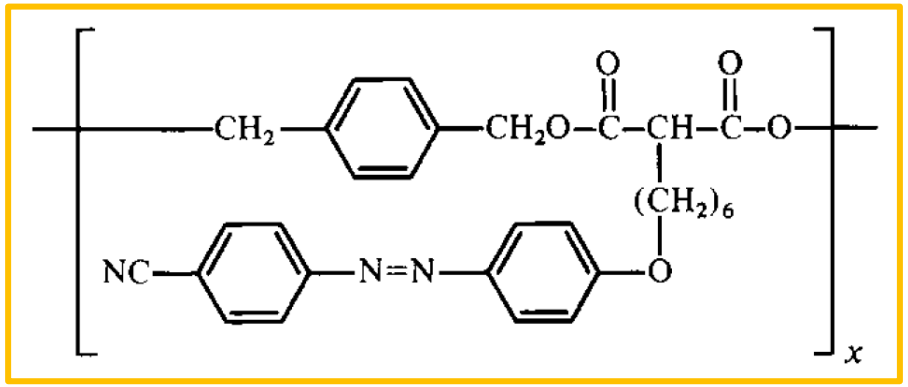

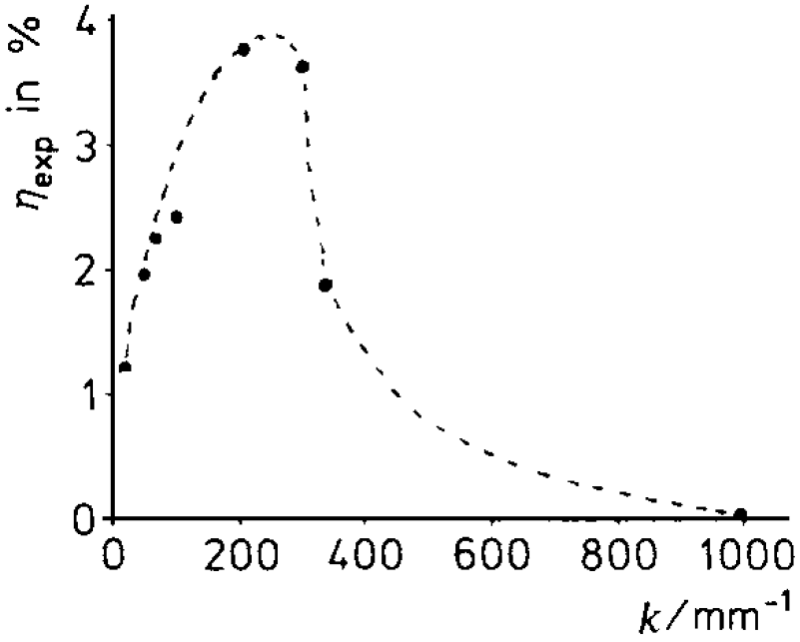

- **Liquid crystalline (LC) side-chain azopolymer (glassy 43° smecticA 94° nematic 104° isotropic)**
- Film thickness ≈ 7 µm
- λ_{rec} = 514.5 nm, I = 100 mW/cm^2; λ_{probe} = 632.8 nm
- Photoinduced birefringence: $\boldsymbol{\Delta n \approx 7.10^{-3}}$
- Diffraction efficiency: $\boldsymbol{\eta \approx 4\%}$
- Thermal erasure (> T_{NI}) and re-writing

Eich et al, Makromol. Chem. Rapid Commun. **8**, 59 (1987)

Azopolymer systems (in search for the perfect azopolymer)

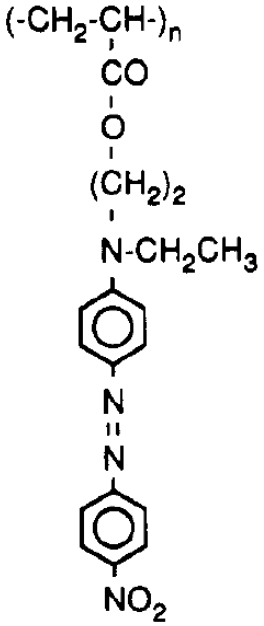

pDR1A Tg = 91°C

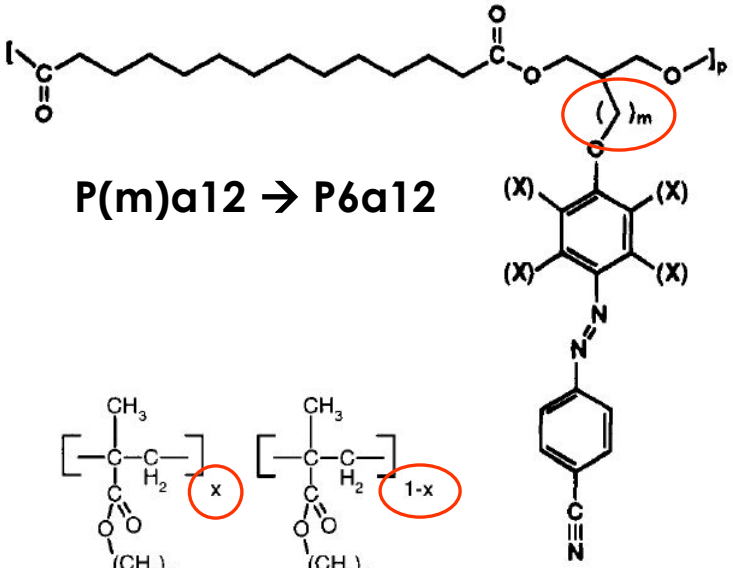

P(m)a12 → P6a12

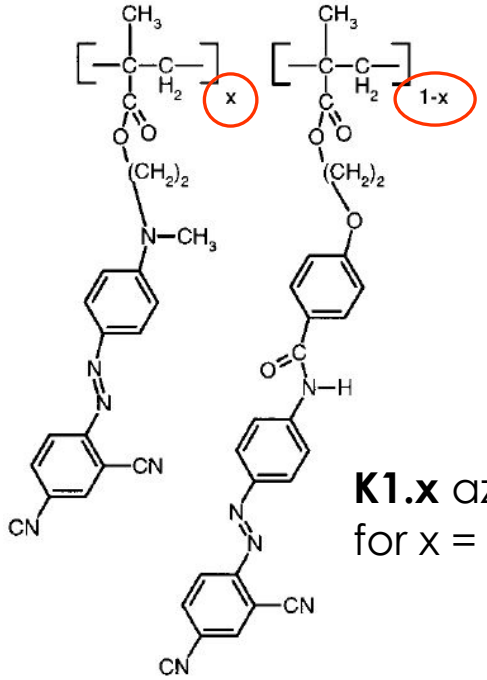

K1.x azopolymers
for x = 40%, **Δn = 0.23**

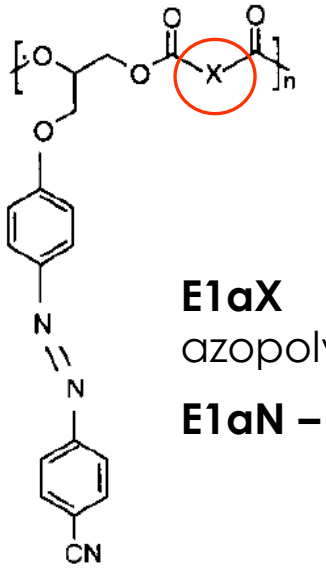

E1aX
azopolymers

E1aN – Δn = 0.13

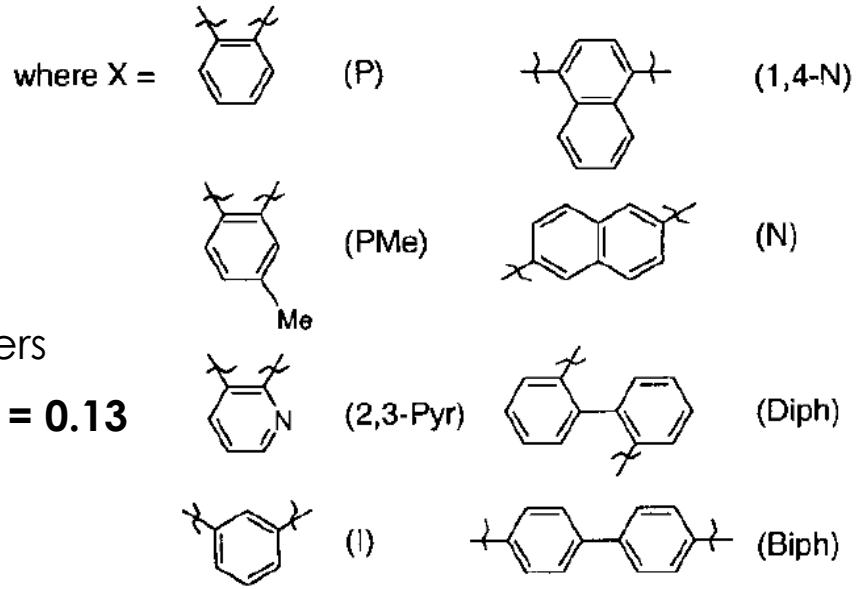

Natansohn et al, Macromolecules **25**, 2268 (1992) – pDR1A
Hvilsted et al, Macromolecules **28**, 2172 (1995) – P6a12
Zilker et al, Adv. Mater. **10**, 855–859 (1998) – K1.x

Nedelchev et al, Appl. Opt. **42**, 5918 (2003) – E1aX
Wang, Azo Polymers: Synthesis, Functions and Applications (2017)

The azopolymer PAZO

poly[1-[4-(3-carboxy-4-hydroxyphenylazo)benzenesulfonamido]-1,2-ethanediyl, sodium salt]

Important advantages:

- Commercially available – allows for verification and reproducibility of results;
- Readily soluble in water and methanol;
- High photoinduced birefringence – $\Delta n \approx 0.08$;
- Excellent thermal stability (>250°C) and very good long-term stability;
- Amorphous azopolymer, excellent optical quality of the thin film samples;

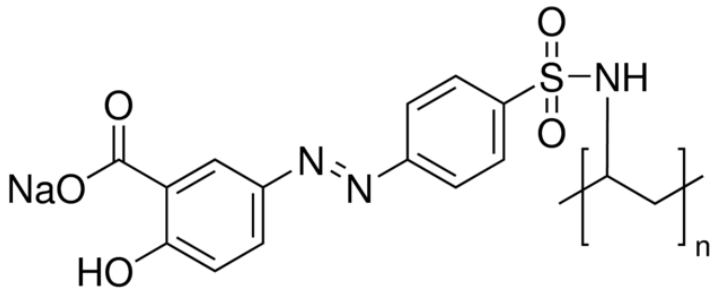

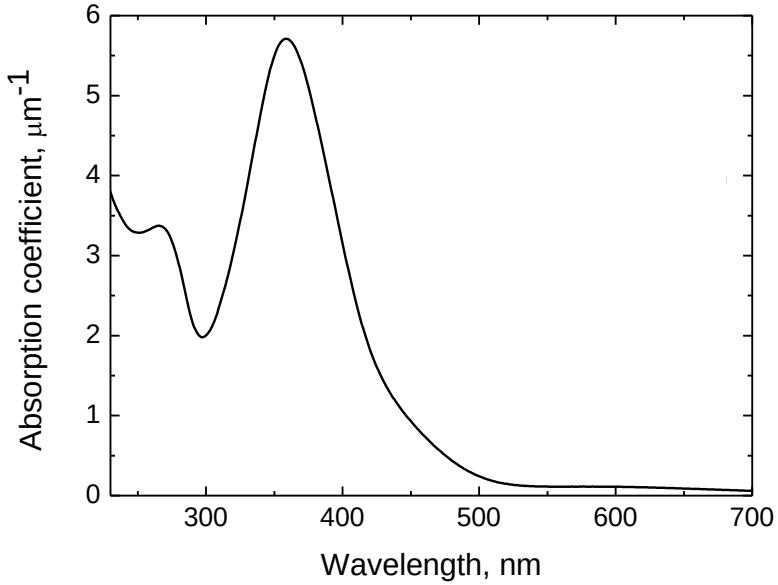

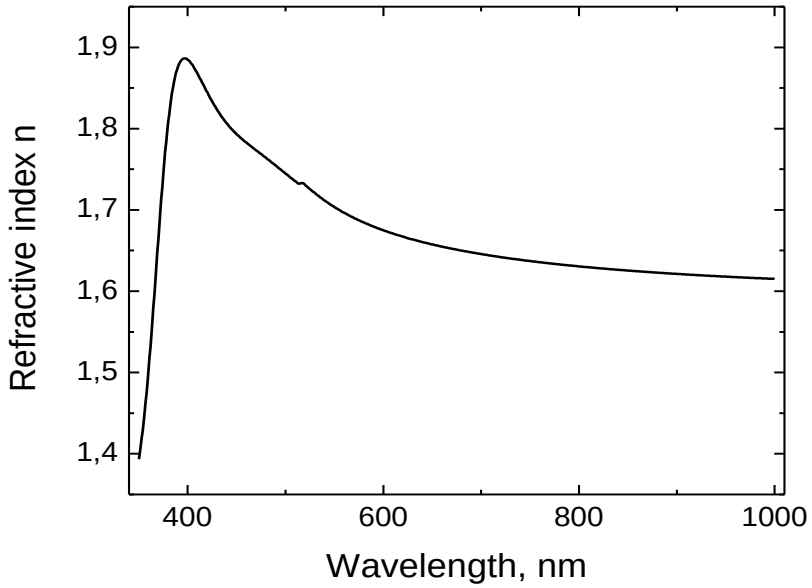

Lvov et al, Thin Solid Films **300**, 107 (1997)
Nedelchev et al, Opt. Quant. Electron. **50**, 212 (2018)
Falcione et al, Opt. Mater. **115**, 111015 (2021)
Minkov et al, Materials **15**, 8617 (2022)

Thickness measurement of thin film samples

The precise measurement of the thickness of the photoanisotropic film samples is necessary in order to determine essential thickness-independent characteristics, as the value of **the photoinduced birefringence** and **the absorption coefficient**.
Different techniques can be used: stylus profilometry, thin film interference method, spectral methods, SEM, AFM, or others.

1. Stylus Profilometry

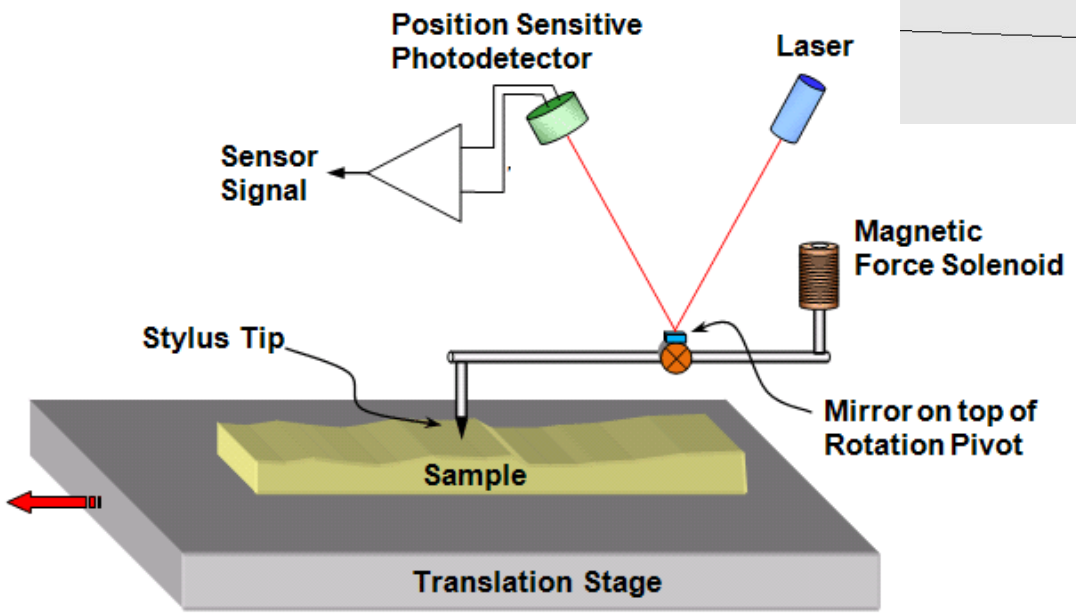

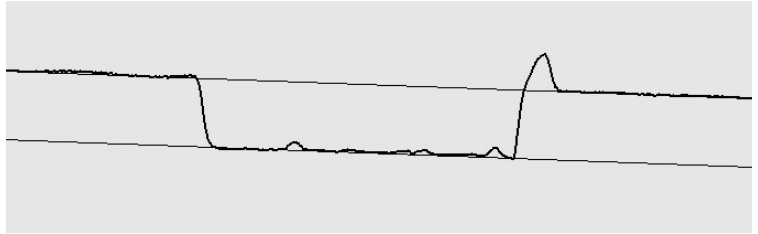

Example of a profilometric scan

Advantages:

- ✓ robust and reliable method;
- ✓ Does not require to know the (n, k) of the film;
- ✓ Broad range: 10 nm – 10 μm

Disadvantage:

- ➢ Requires to remove a strip of the photoanisotropic film

https://australiasurfacemetrologylab.org/new-page

Thickness measurement of thin film samples

2. Interferometric method

The method is based on the interference of light reflected from the upper and lower boundaries of the thin film.

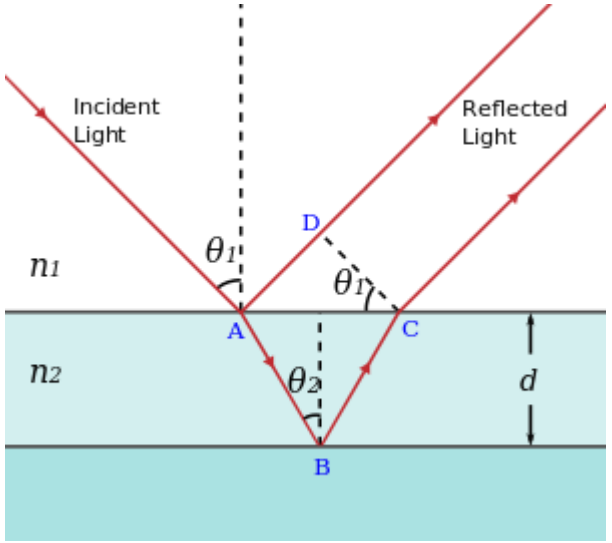

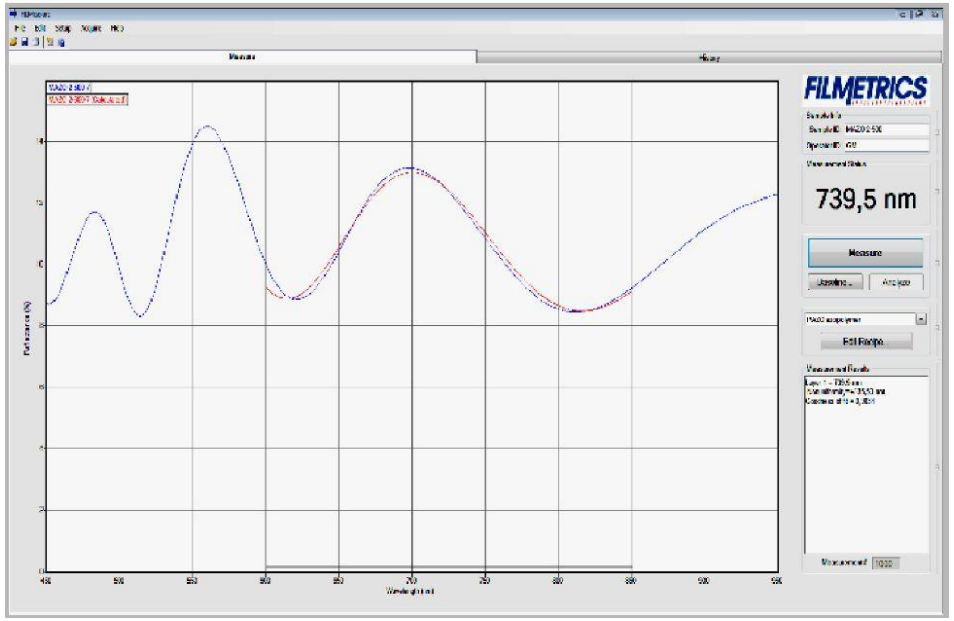

Advantages:

- ✓ Fast and non-destructive method;
- ✓ Measurement spot size matches the holographic recording spot (d~5 mm)

Limitations:

- ➢ Requires to know the (n, k) of the film
- ➢ Film has to be transparent, uniform and non-scattering

Nedelchev et al, Int. J. Inf. Theor. Appl. **25**, 245 (2018)

Photoinduced birefringence measurement
(crossed polarizers and polarimetric setup)

- fast and simple way to determine the material's potential for polarization holographic applications
- no vibro isolation is required
- lasers don't have to be coherent, even LEDs can be used as pump light source

1. Crossed polarizers setup

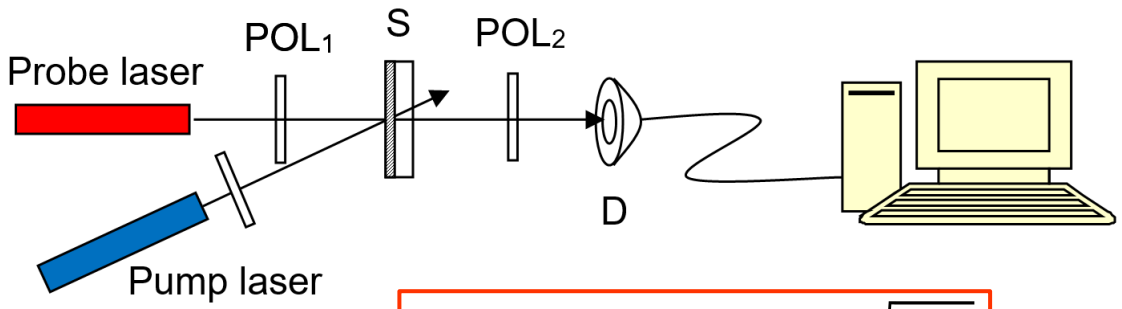

$$\Delta n(t) = \frac{\lambda_{probe}}{\pi d} \arcsin \sqrt{\frac{I(t)}{I_0}}$$

d – film thickness
$\boldsymbol{\lambda_{probe}}$ – wavelength of the probe laser
$\boldsymbol{I_0}$ – intensity at parallel polarizers before exposure
I(t) – intensity at crossed polarizers during the exposure

2. Polarimetric setup

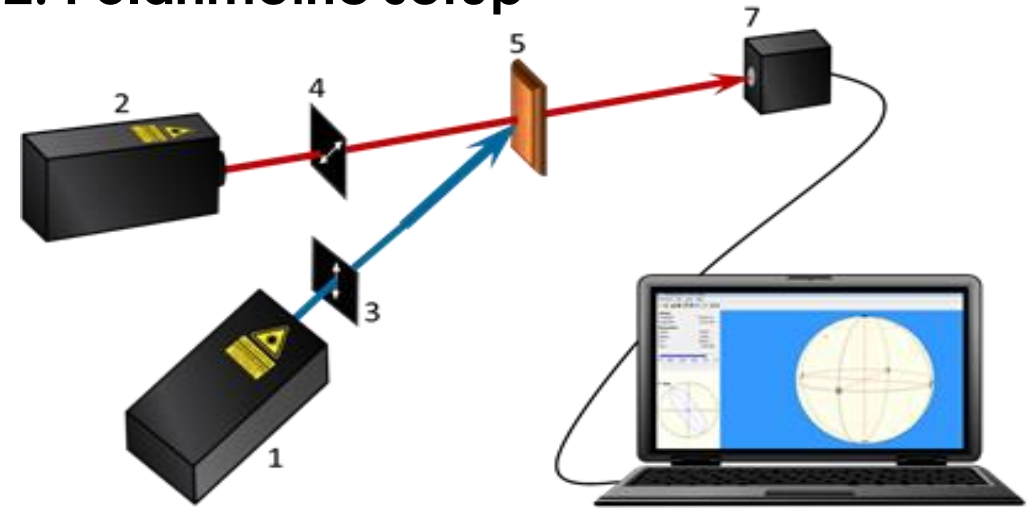

$$\Delta n(t) = \frac{\lambda_{probe}}{2\pi d} \arctan \sqrt{\frac{S_3(t)}{S_2(t)}}$$

$\mathbf{S_0}$, $\mathbf{S_1}$, $\mathbf{S_2}$, $\mathbf{S_3}$ – Stokes parameters

The dichroism value can also be determined:

$$\Delta D = \lg \frac{S_0 + S_1}{S_0 - S_1}$$

Parameters of the photoinduced birefringence
(derived from the birefringence kinetics curve)

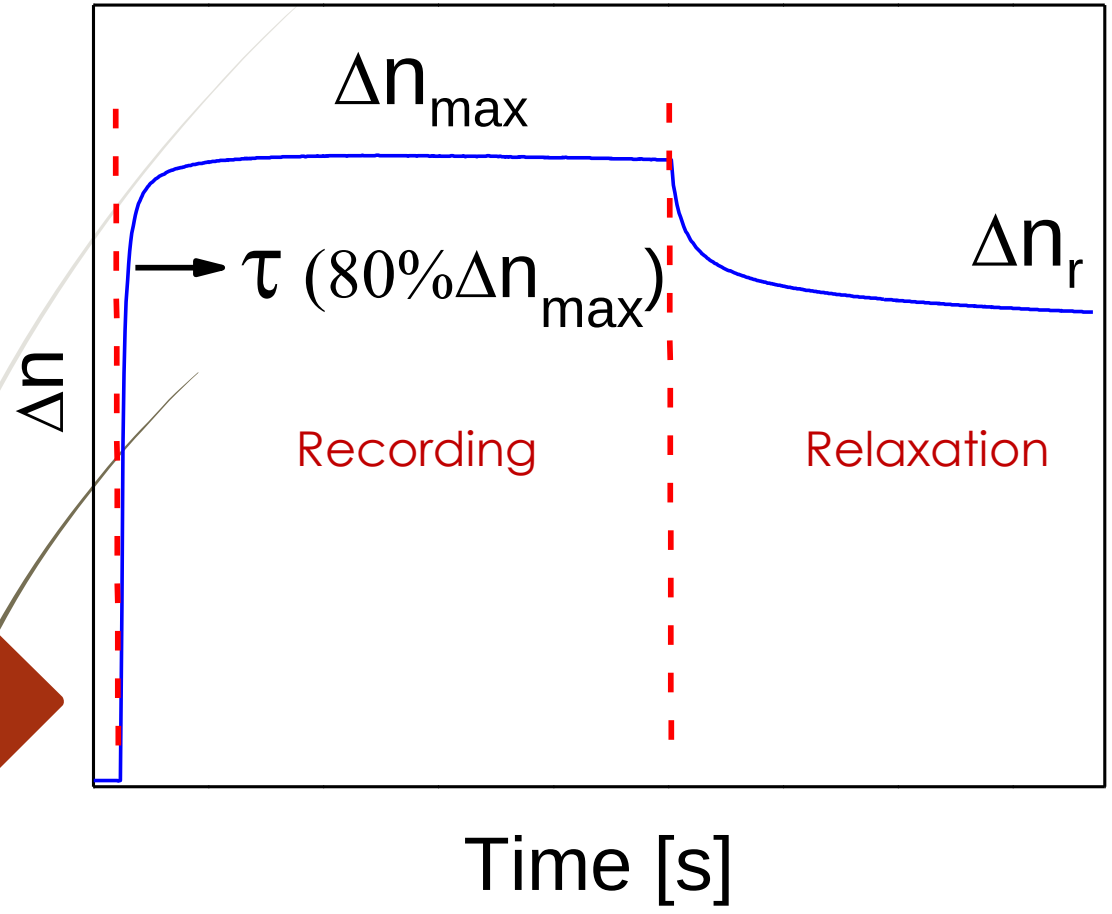

- Maximal value of the photoinduced birefringence – $\boldsymbol{\Delta n_{max}}$
- Response time – $\boldsymbol{\tau}$ (time to reach 80% of Δn_{max})*
- Time stability – $\boldsymbol{r} = \frac{\Delta n_r}{\Delta n_{max}}$

The value of Δn_{max} allows to estimate the diffraction efficiency (η) that can be achieved in the sample, using Kogelnik's formula:

$$\eta = \sin^2\left[\frac{\pi \Delta n d}{\lambda}\right]$$

* The birefringence kinetics can be also fitted with **biexponential** curve, however it is described with four parameters, instead of one.

$$\Delta n(t) = \Delta n_{slow}(1 - e^{-k_{slow} t}) + \Delta n_{fast}(1 - e^{-k_{fast} t})$$

Ho et al, Macromolecules **28**, 6124 (1995)
Nedelchev et al, Appl. Opt. **42**, 5918 (2003)

Optimal recording wavelength selection

(based on the photoinduced birefringence for the azopolymer PAZO)

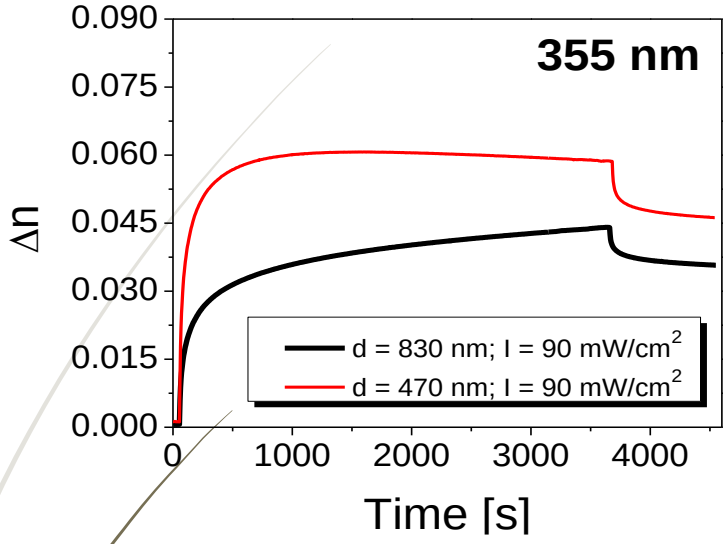

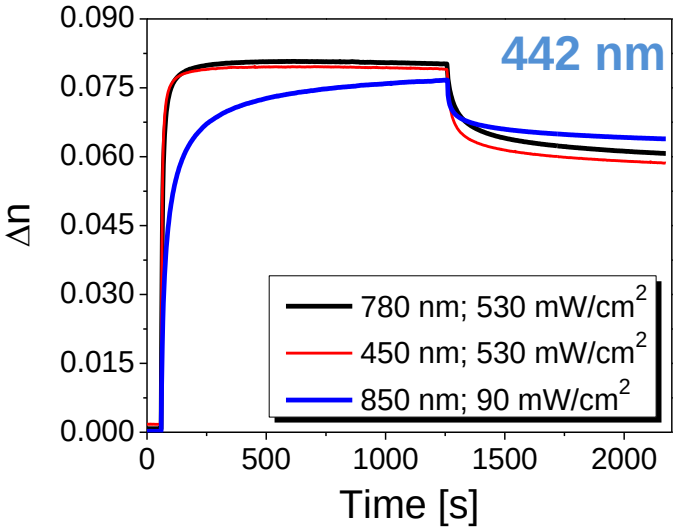

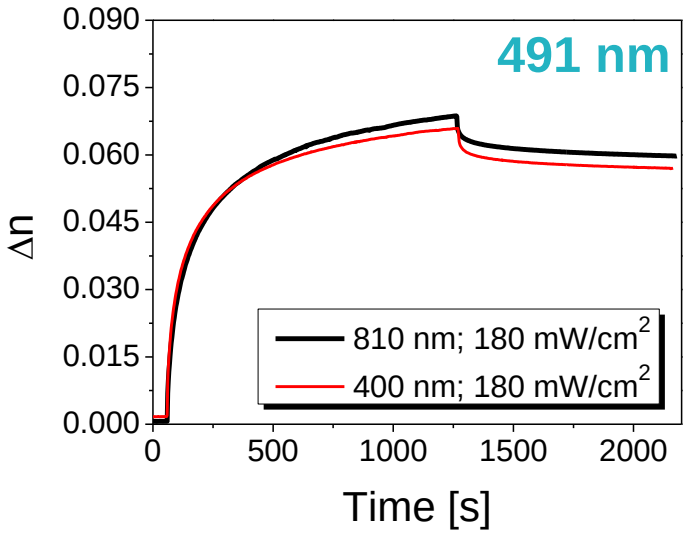

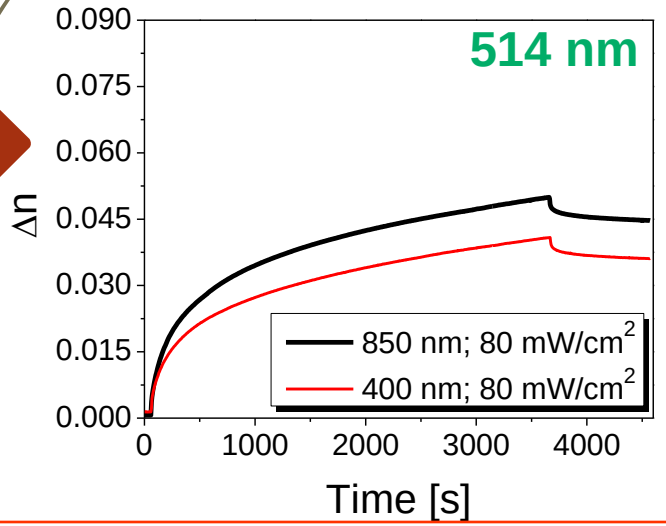

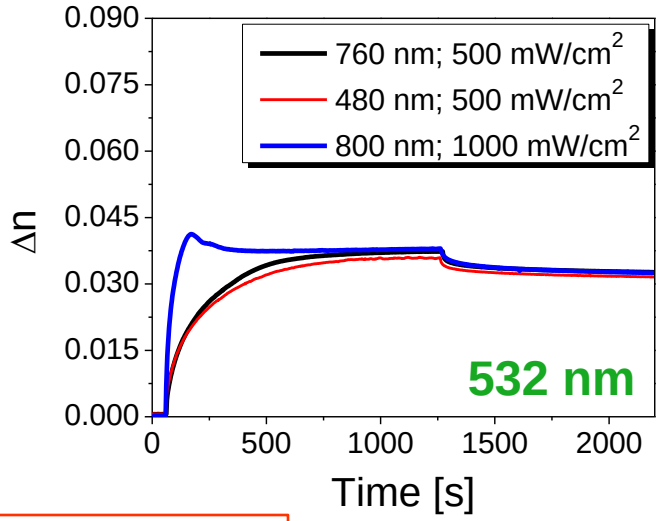

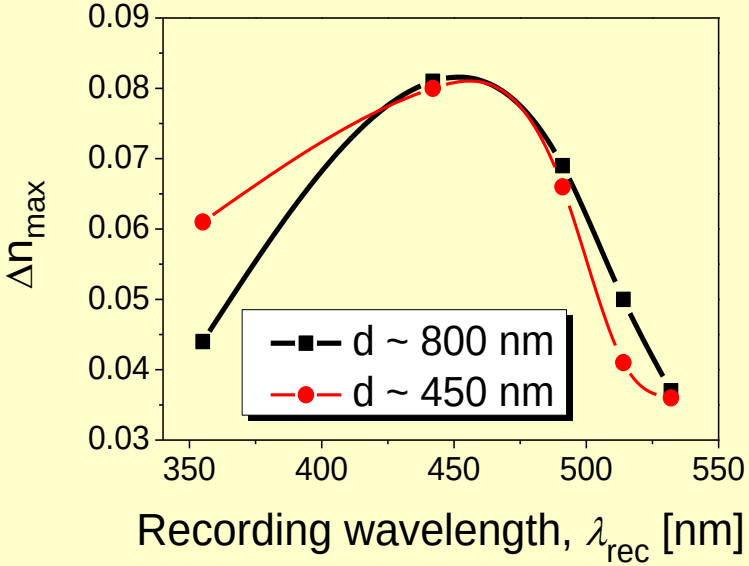

Nedelchev et al, J. Photochem. Photobiol. A: Chem. **376**, 1 (2019)

Optimal recording wavelength selection
(parameters of the photoinduced birefringence for PAZO)

λ_{pump} [nm]	d [nm]	I [mW/cm^2]	Δn_{max}	τ [s]	r_{15min} [%]
355	830	90	0.044	840	81.2
	470		0.061	160	78.7
442	780	530	0.081	15	75.7
	450		0.080	10	74.2
	850	90	0.077	106	83.3
491	810	180	0.069	320	87.0
	400		0.066	270	86.5
514	850	80	0.050	1560	89.4
	400		0.041	1710	88.0
532	760	500	0.037	280	87.4
	480		0.036	300	87.8
	800	1000	0.041	50	87.1

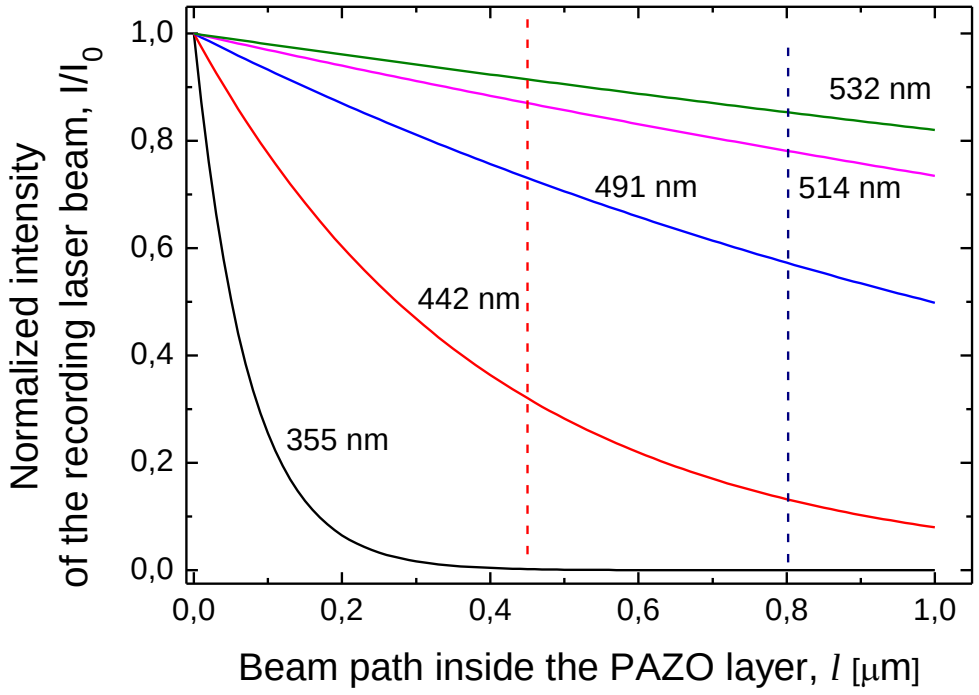

Note: The recording beam intensity inside the film is NOT constant. For wavelengths close to the absorbance peak of the material, the decrease in intensity could be significant.

Nedelchev et al, J. Photochem. Photobiol. A: Chem. **376**, 1 (2019)

Birefringence measurement in a broad spectral range

Transmission spectra $T(\lambda)$ are measured, before exposure with sample placed between:

1) parallel polarizers – $T_{\parallel}^{non-exp}(\lambda)$

2) crossed polarizers – $T_{\perp}^{non-exp}(\lambda)$

and after exposure

3) between crossed polarizers – $T_{\perp}^{exp}(\lambda)$

$$\Delta n(\lambda) = \frac{\lambda}{\pi d} \arcsin \sqrt{\frac{T_{\perp}^{exp} - T_{\perp}^{non-exp}}{T_{\parallel}^{non-exp}}}$$

Note: In this case the wavelength in the equation is **not** constant.

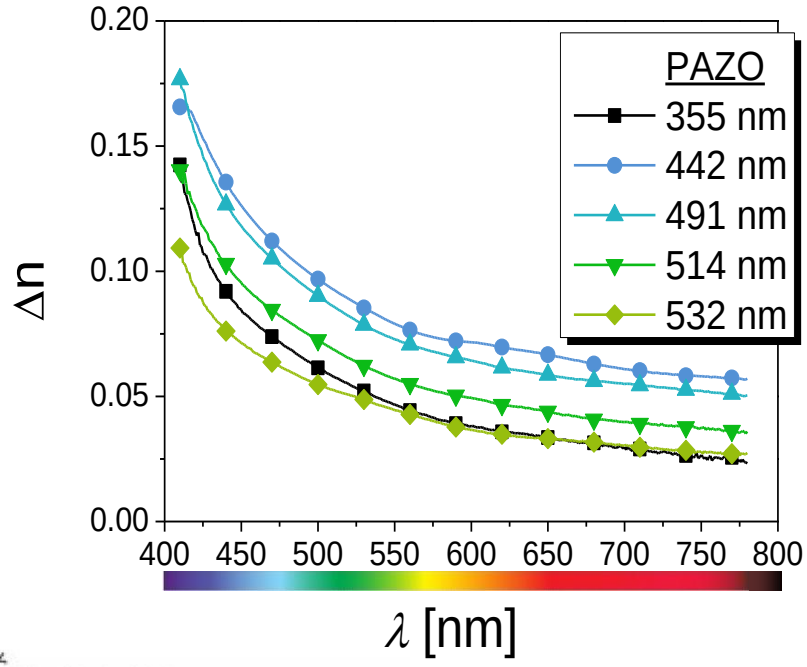

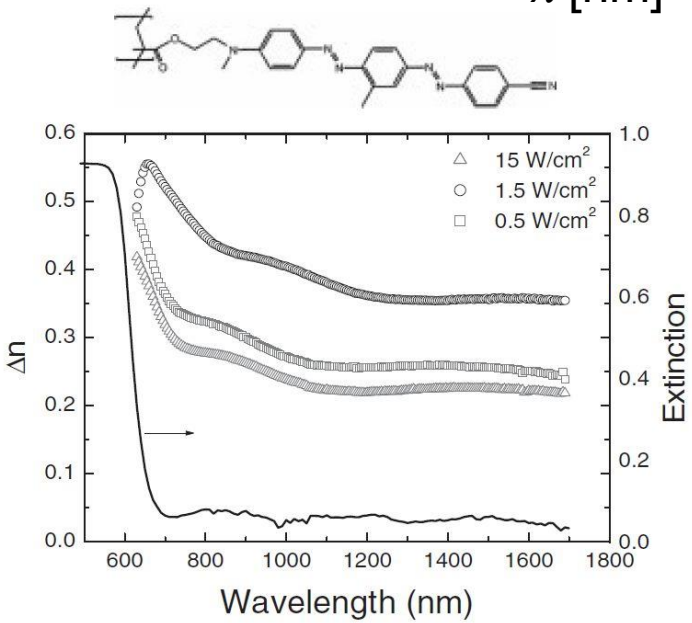

Lachut et al, Adv. Mater. **16**, 1746 (2004)
Nedelchev et al, J. Photochem. Photobiol. A: Chem. **376**, 1 (2019)

Reversibility of the photoinduced birefringence (thermal erasure)

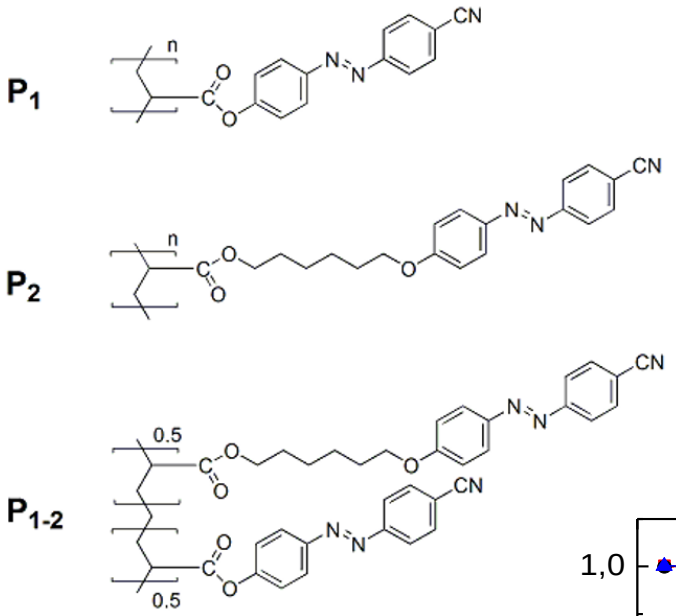

The samples were mounted on a heating stage:

- starting temperature – 25 °C
- speed of heating – 5°C/min

The anisotropy for the **P_1**, **P_{1-2}** and **P_2** polymers is fully erased at **85–130°C**.

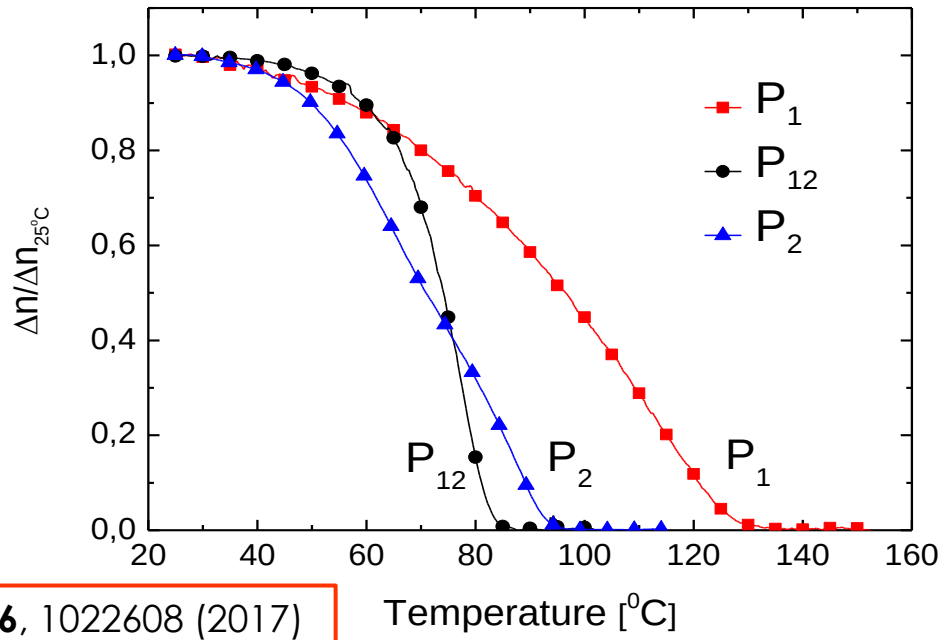

The erasing temperature for **PAZO** is more than **300°C**.

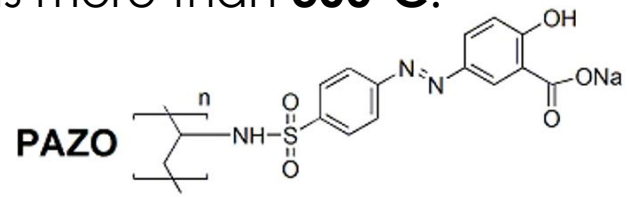

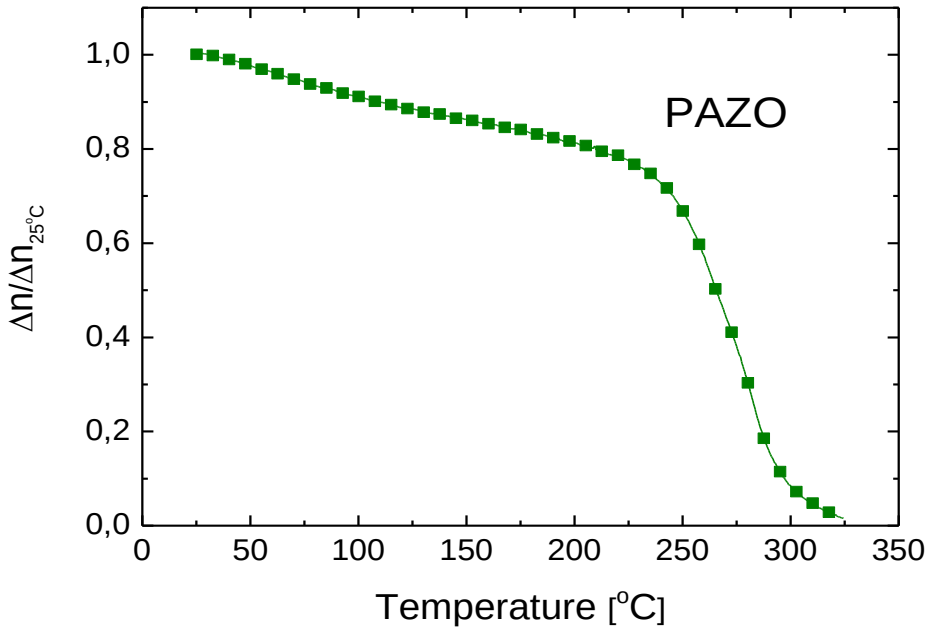

Nazarova et al, Proc. SPIE **10226**, 1022608 (2017)

Reversibility of the photoinduced birefringence
(thermal *vs.* optical erasure and re-recording)

Multiple cycles of recording/reading/ erasing birefringence using optical or thermal erasure in the azopolymer P_{1-2}.

The decrease is due to the orientation of the chromophores perpendicular to the plane of the film.

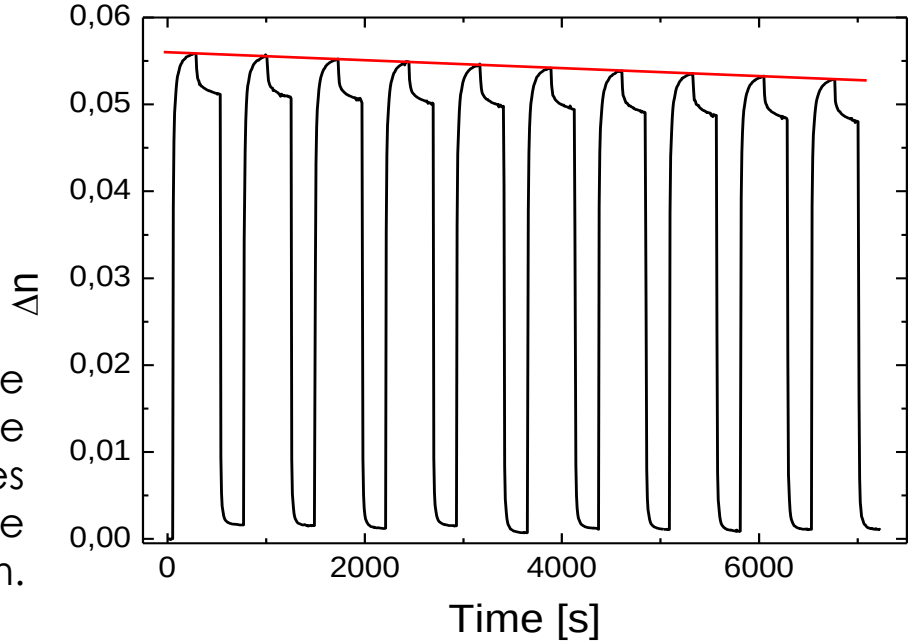

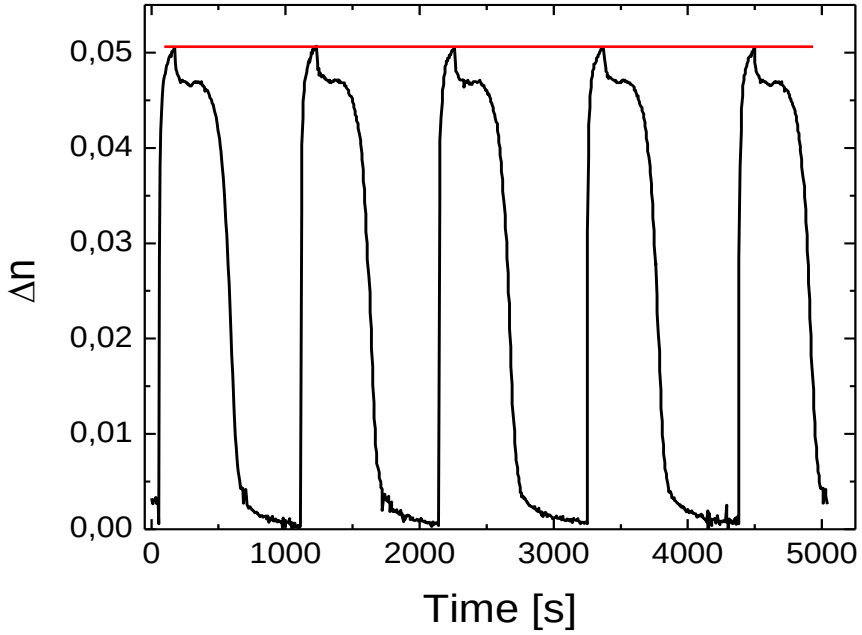

Optical erasure

by irradiation with **circularly polarized** or **non-polarized** light

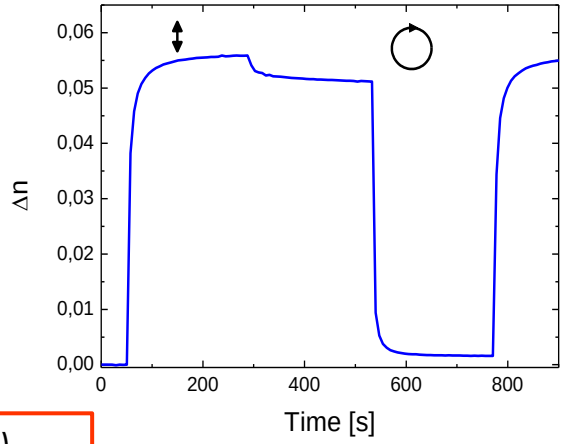

Thermal erasure

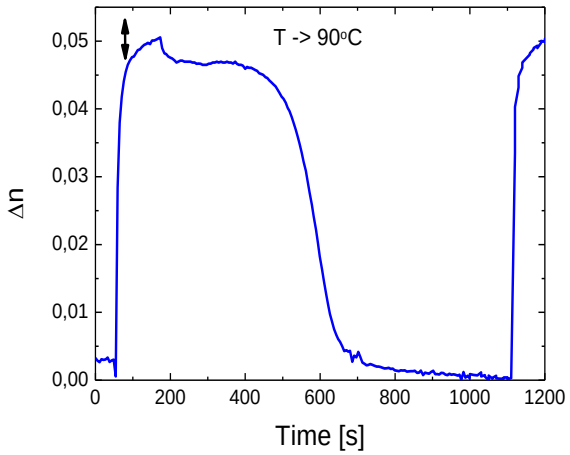

Nedelchev et al, Bulg. Chem. Commun. **48**, 33 (2016)

Azopolymer nanocomposites

azopolymer

+

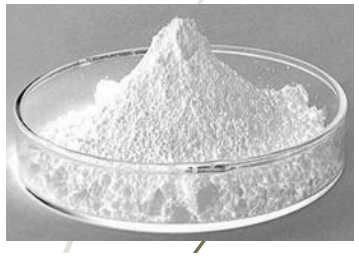

nanoparticles

=

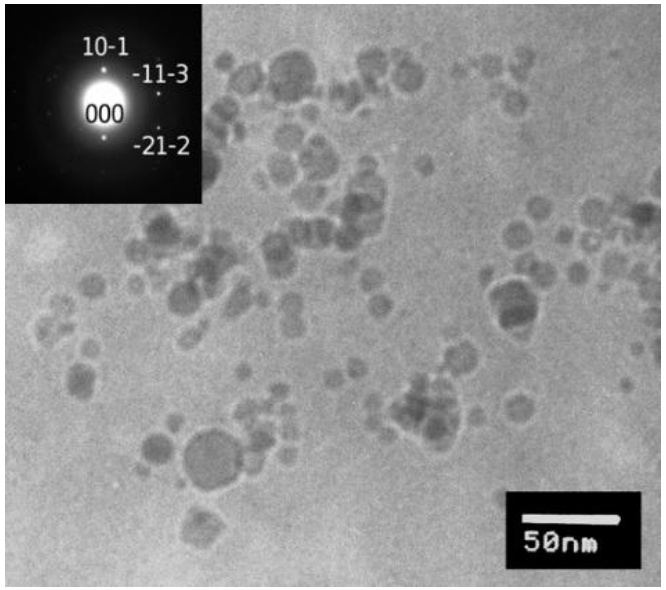

Azopolymer doped with ZnO nanoparticles

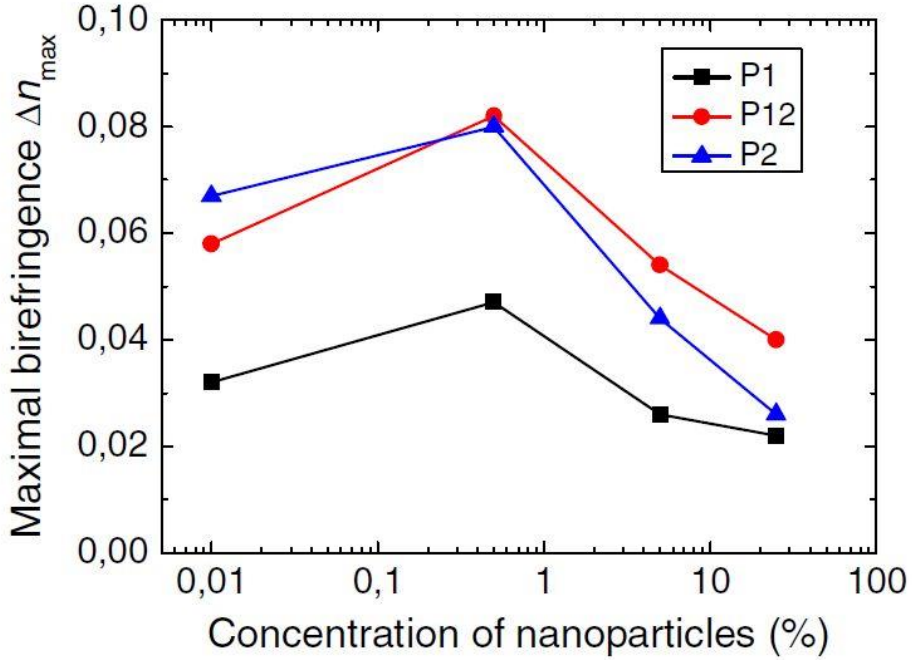

For P1 doped with **0.5%** ZnO NP, a **47%** increase of the birefringence is observed.

	Maximal Value of the Photoinduced Birefringence Δn_{max}					Response Time $\tau(s)$				
NP Concentration (%)	0	0.5	5	25	Maximal Increase of Δn_{max}	0	0.5	5	25	Maximal Decrease of τ
$\mathbf{P_1}$ ($M_w = 14\,600$, $T_g = 106\,°C$)	0.032	0.047	0.026	0.022	47%	22	16	20	21	27%
$\mathbf{P_{1-2}}$ ($M_w = 3600$, $T_g = 102\,°C$)	0.058	0.082	0.054	0.040	41%	14	12	11	10	29%
$\mathbf{P_2}$ ($M_w = 2050$, $T_g = 35\,°C$)	0.067	0.080	0.044	0.026	19%	12	23	17	13	—

Nedelchev et al, Opt. Lett. **37**, 2676 (2012)

Ingredients of the nanocomposite materials

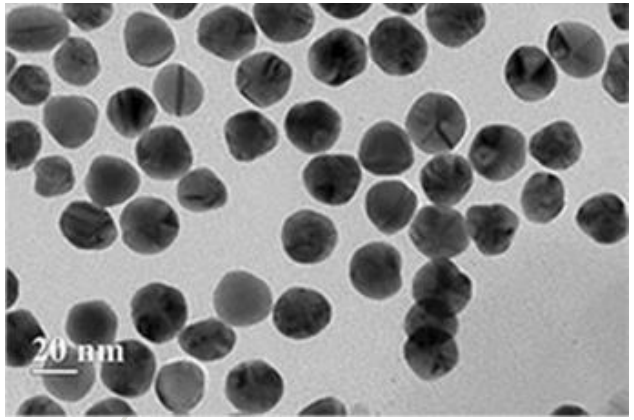

Gold nanospheres 20nm

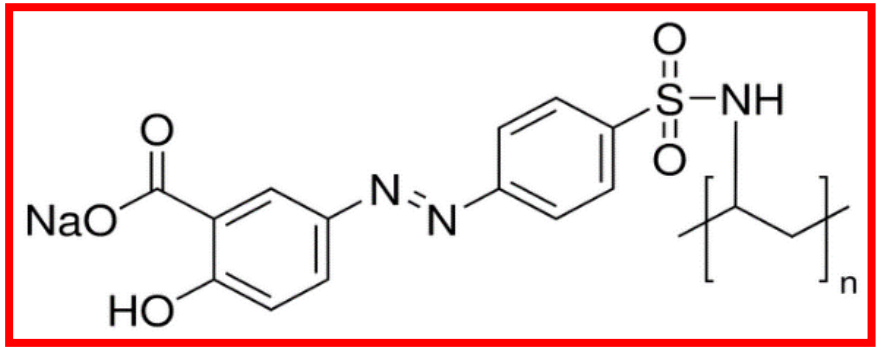

Azopolymer PAZO (Sigma Aldrich)

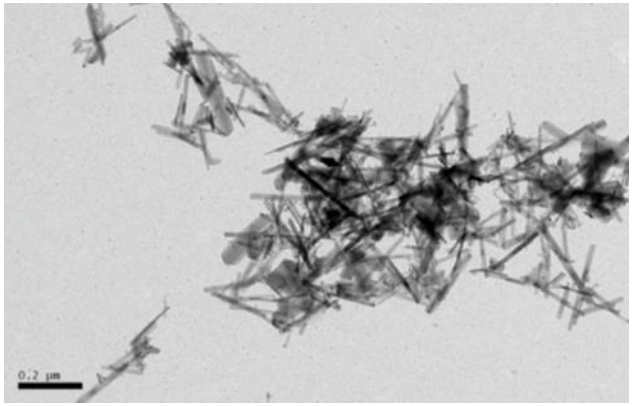

Goethite nanorods

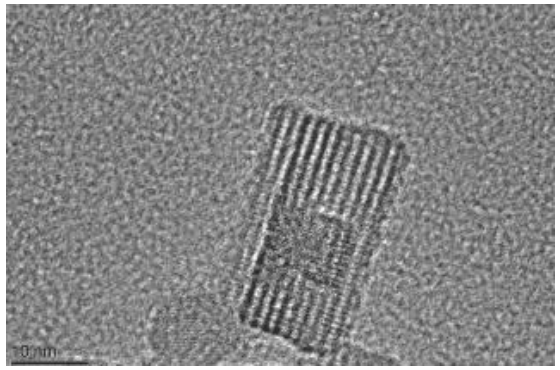

MFI (Mordenite Framework Inverted) zeolite NP

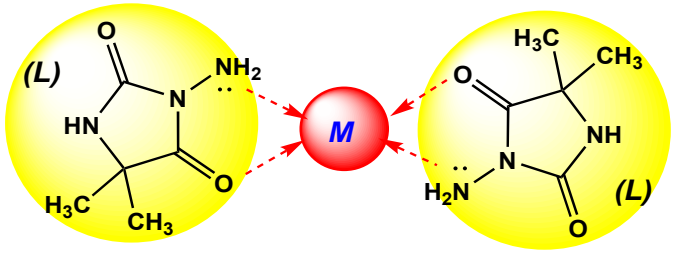

M = Cu^{2+} or Ni^{2+}

Bioactive metal complexes

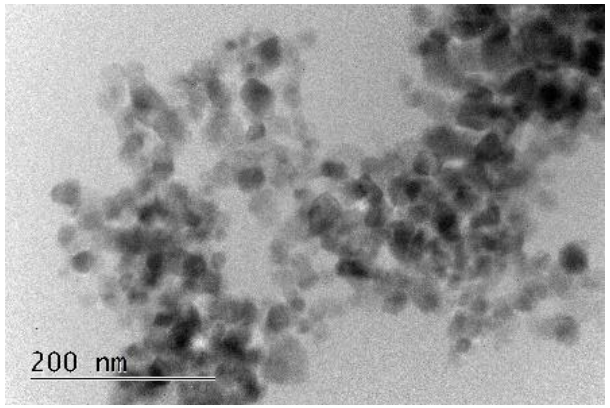

TiO_2 nanoparticles

Azopolymer nanocomposites

PAZO with goethite (a-FeOOH) nanorods

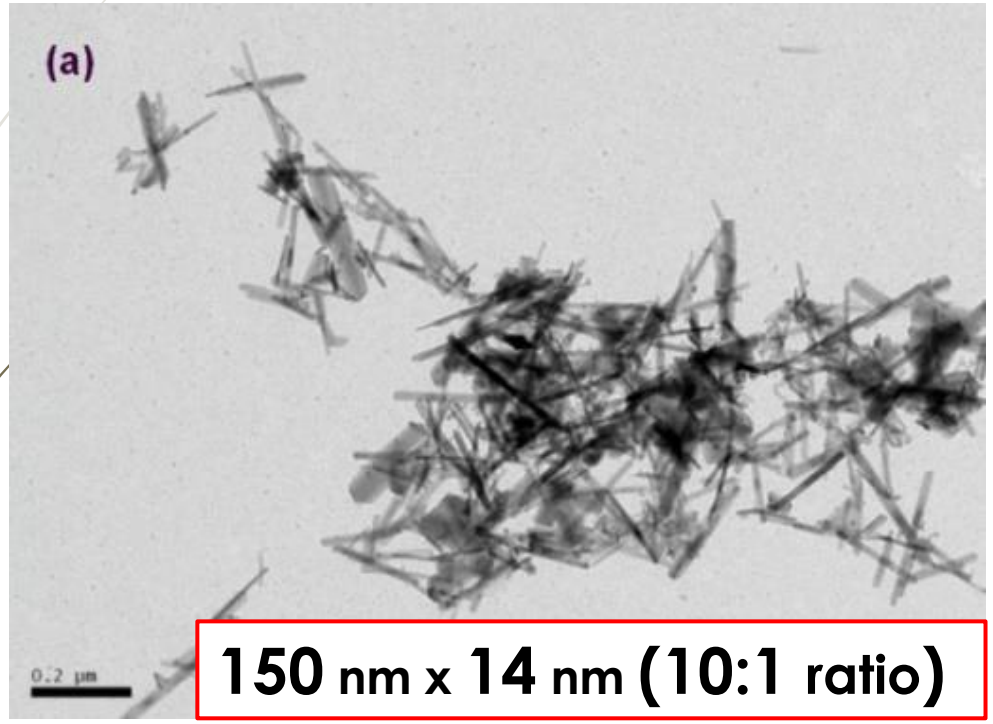

150 nm x 14 nm (10:1 ratio)

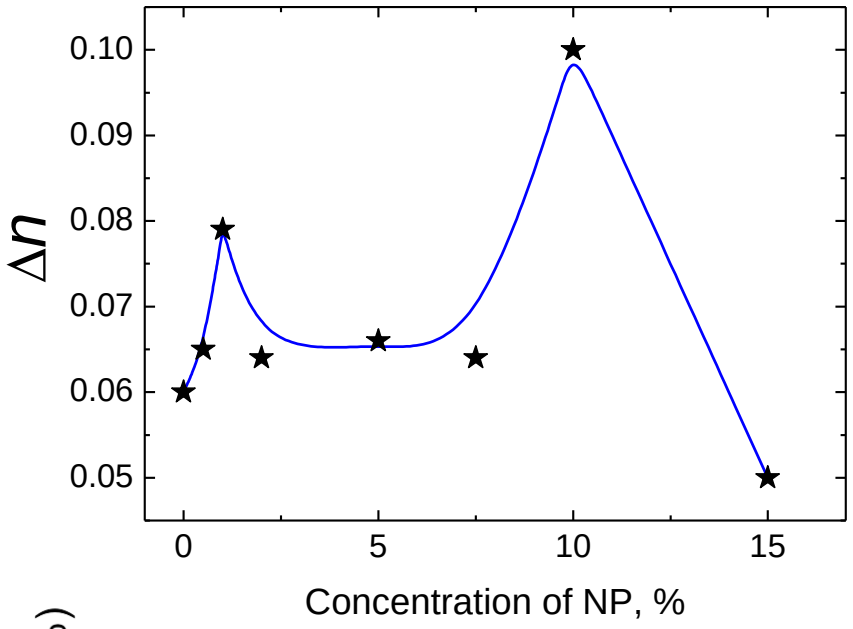

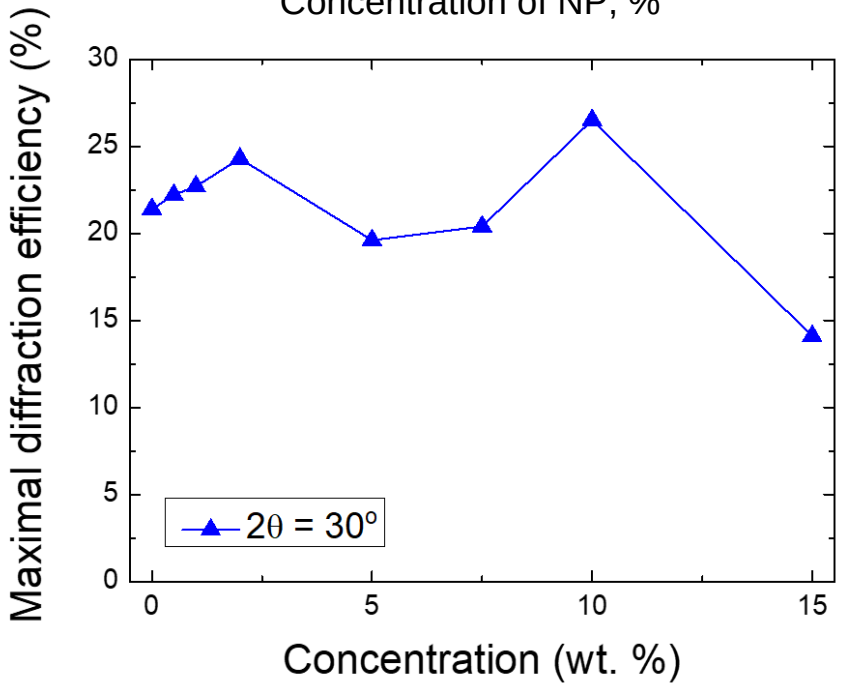

Nedelchev et al, J. Phys. Conf. Ser. **700**, 012031 (2016)
Nedelchev et al, Photonics **8**, 306 (2021)

Hypotheses for the enhancement of the birefringence in nanocomposites

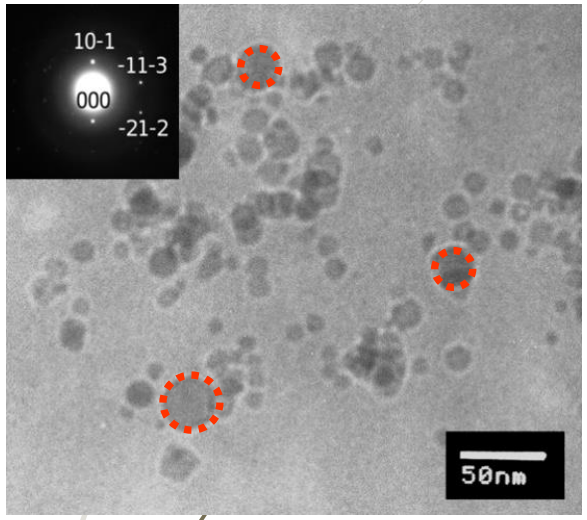

1. Free volume increase around the nanoparticles leading to higher mobility of the azochromophores.

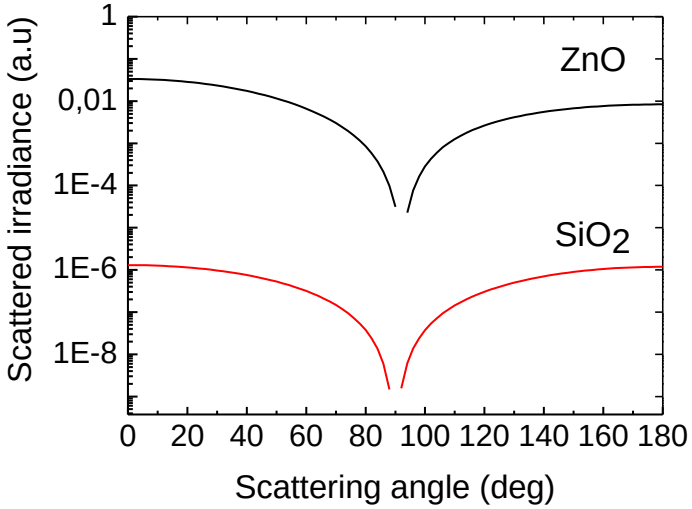

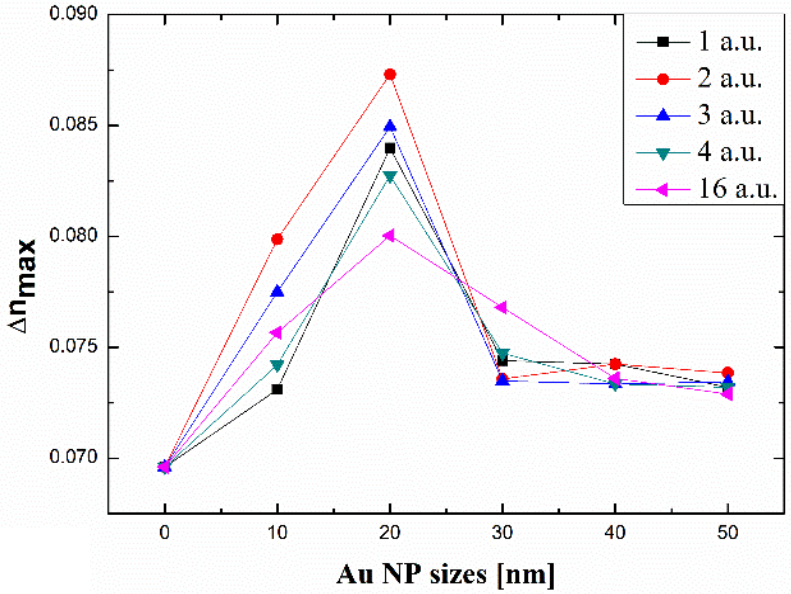

2. Scattering of light allows to address azomolecules oriented perpendicular to the plane of the film.

Our experiments with Au NP with varying sizes indicate that the "free volume" effect is more significant.

Nazarova et al, Appl. Opt. **52**, E28 (2013)
Berberova-Buhova et al, Opt. Mater. **121**, 111560 (2021)

PQ/PMMA – a photoanisotropic photopolymer
(phenanthrenequinone-doped poly(methyl methacrylate))

- **1991** – First description;
- Initially used for traditional holographic storage at 488/514 nm; recording process: photoaddition of PQ to MMA
- **2000** – 250 holograms at 514.5 nm, M/# = 14;
- **2009** – $\Delta n = 1.4 \times 10^{-4}$ at RT, $\Delta n = 2.2 \times 10^{-4}$ at 58°C (λ_{pump} = 436 nm)
- **2011** – DE ≈ 40% (RCP+LCP)
- **2013** – DE ≈ 70% (PQ/DMNA) Δn (PQ/DMNA) = 2.1×10^{-3} (λ_{rec} = 532 nm)

Veniaminov et al, Opt. Spectrosc. **70**, 505 (1991)
Lin et al, Opt. Lett. **25**, 451 (2000)
Trofimova et al, J. Appl. Spectrosc. **76**, 585 (2009)
Lin et al, Opt. Lett. **36**, 3039 (2011)
Ko et al, J. Appl. Polym. Sci **127**, 643 (2013)

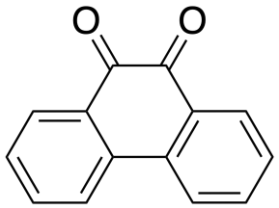

phenanthrenequinone

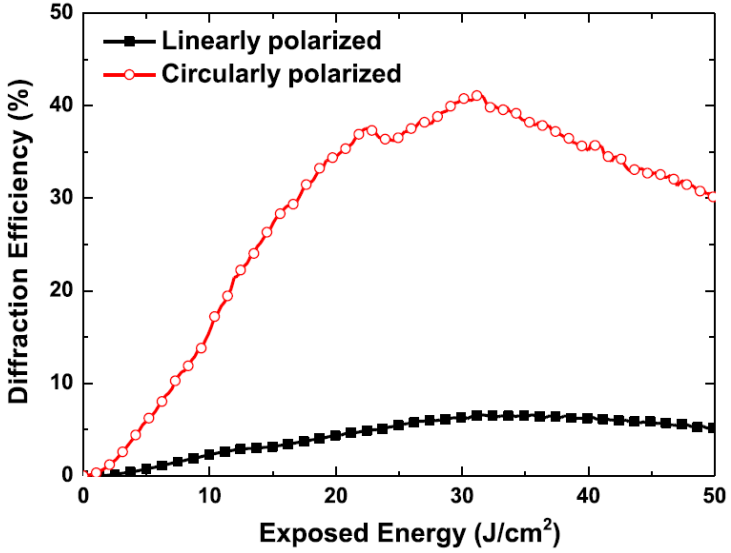

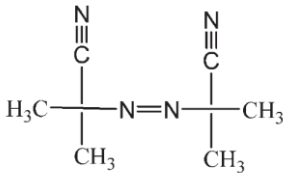

2,2-azo-bis-isobutyrolnitrile (AIBN)

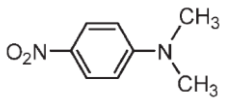

N,N-dimethyl-4-nitroaniline (DMNA)

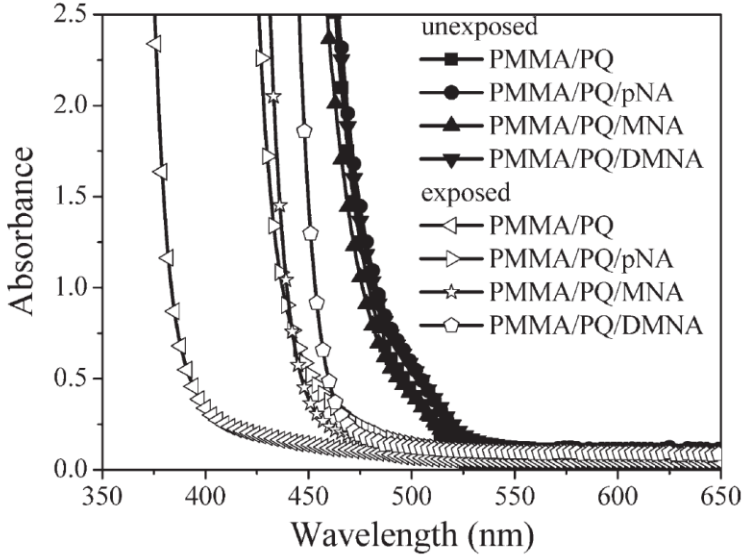

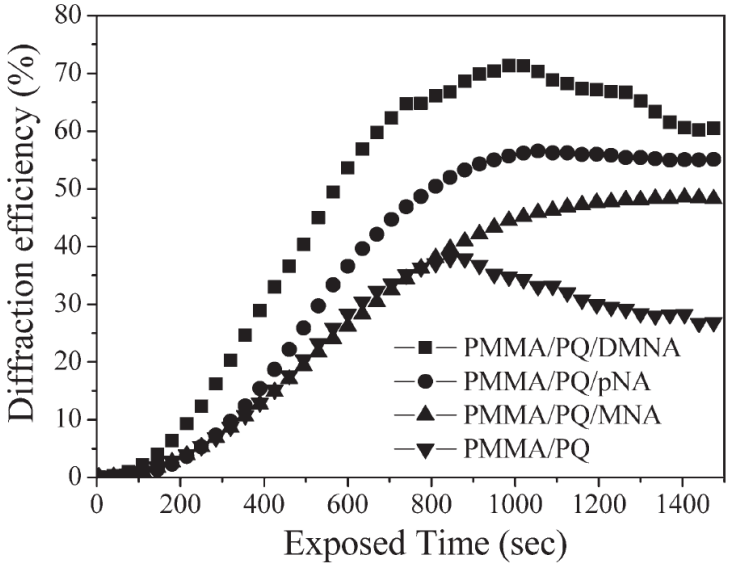

Photoanisotropic materials, transparent in the visible range

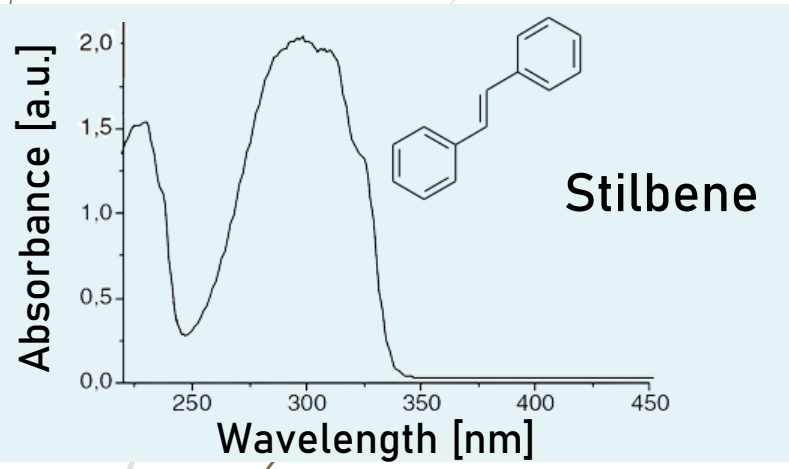

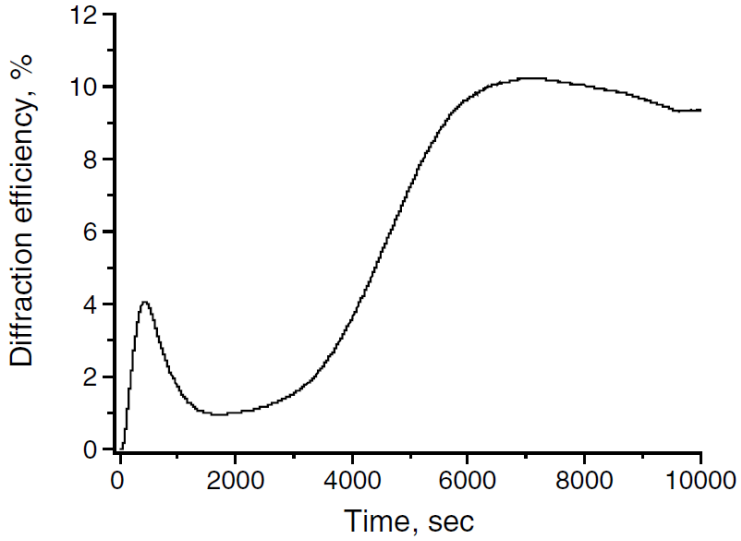

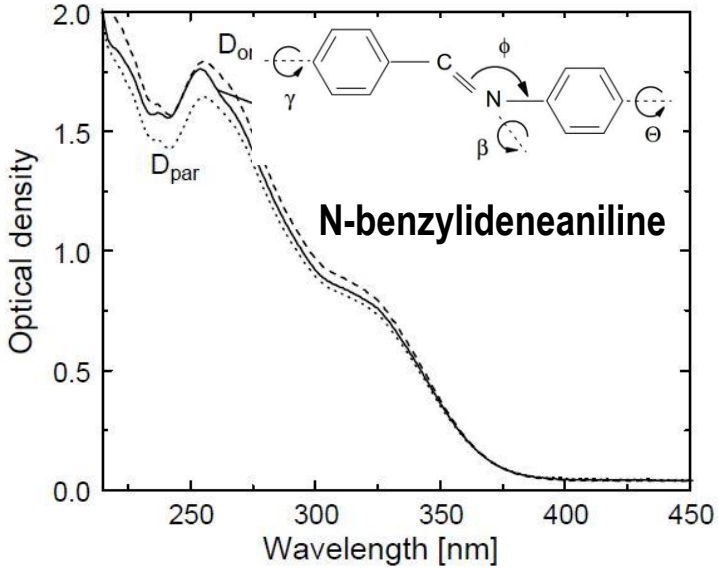

Recording:

- λ_{rec} = 257 nm, I = 160 - 400 mW/cm^2

Challenges:

- powerful and coherent **UV** laser is required
- Low efficiency

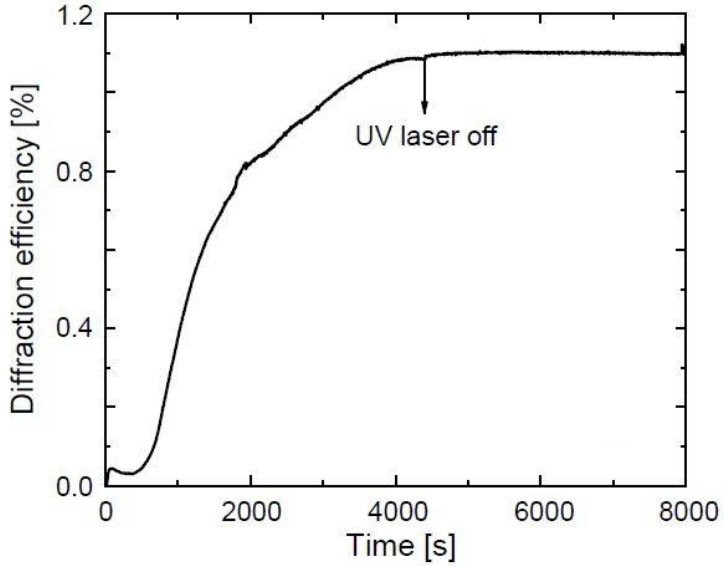

Imamura et al, J. Polym. Sci. B **38**, 682 (2000)
Ilieva et al, J. Opt. A: Pure Appl. Opt. **8**, 221 (2006)
Ilieva et al, Opt. Appl. **42**, 207 (2012)

Important applications:
Polarization-selective diffractive optical elements, surface relief gratings, digital polarization holography

Circular polarization beam splitter for spectrophotopolarimetry

1992

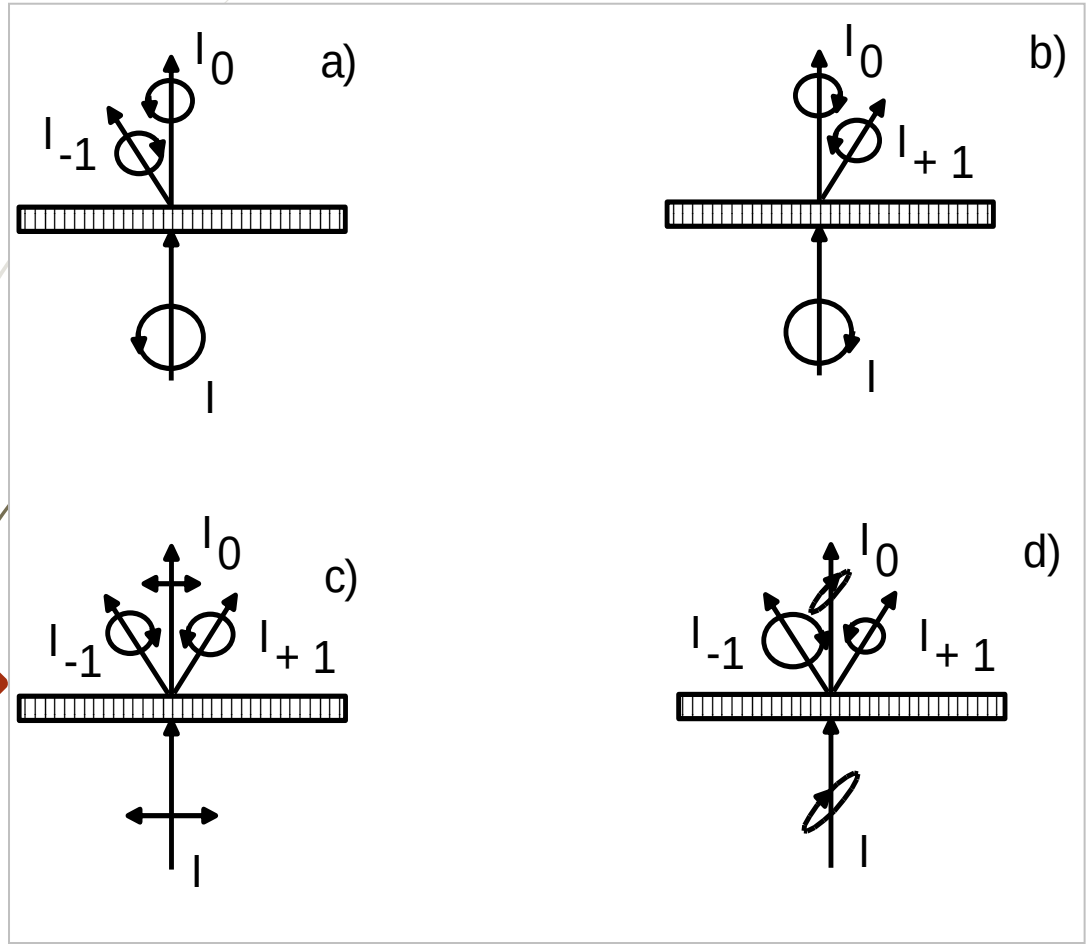

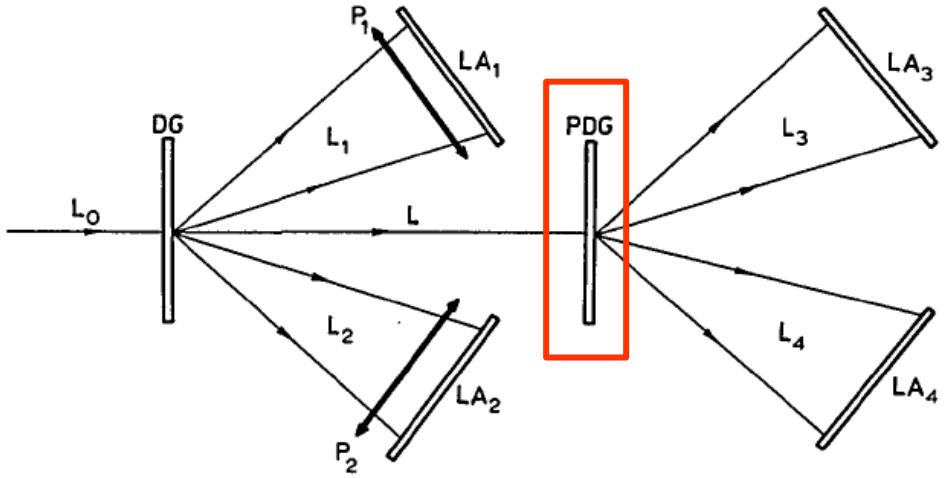

DG – diffraction grating

PDG – polarization diffraction grating

The polarization diffraction grating, acting as circular polarization beam splitter is:

- recorded with left and right circularly polarized waves (LCP and RCP);
- separates the two **circular** components of light (left & right) in +1 and -1 diffracted orders;
- operates in a broad spectral range;

T. Todorov, L. Nikolova, Opt. Lett. **17**, 358 (1992)
T. Todorov et al, Appl. Opt. **46**, 6662 (2007)

Surface relief gratings (SRG) in azopolymers

1995

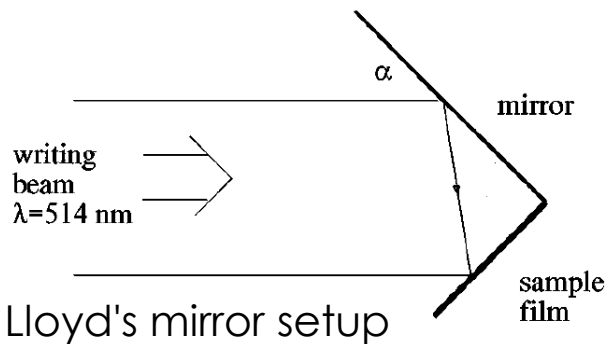

Lloyd's mirror setup

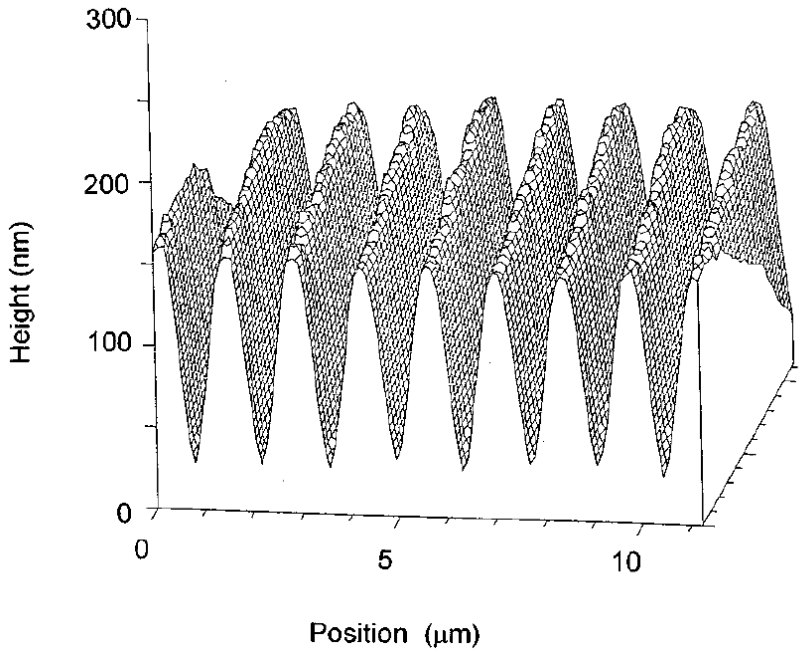

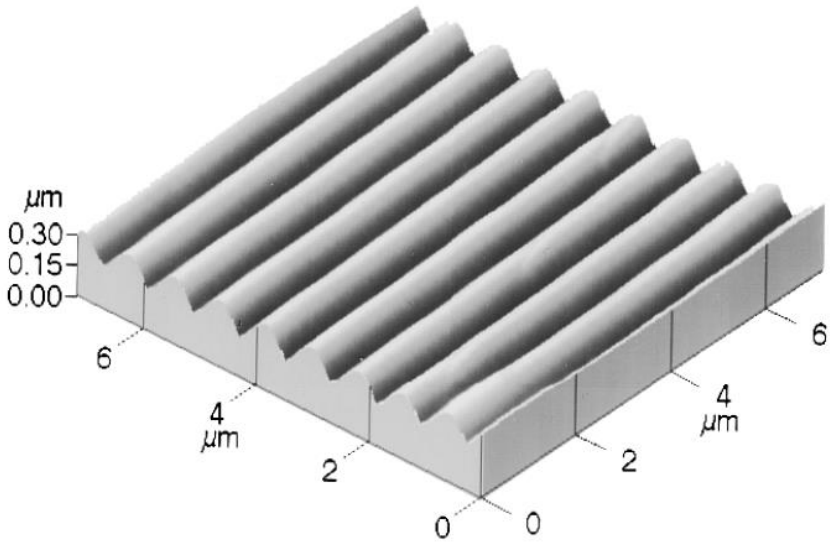

- **Azopolymer pDR1A**
- Film thickness ≈ 400 nm
- λ_{rec} = 514.5 nm, I = 70 mW/cm^2; CP
- Diffraction efficiency: $\boldsymbol{\eta}$ ≈ **28%**
- Λ = 360 – 1000 nm; h_{SRG} ≈ 150-200 nm

- **Epoxy-based polymer** with 4-(4'-nitrophenylazo)phenylamine
- Film thickness ≈ 600 nm
- λ_{rec} = 488 nm, I = 70 mW/cm^2; p-p
- Diffraction efficiency: $\boldsymbol{\eta}$ ≈ **2-5%** (with gold coating: η ≈ 30%)
- Λ = 500 – 2300 nm; h_{SRG} ≈ 120 nm

Rochon et al, Appl. Phys. Lett. **66**, 136 (1995)
Kim et al, Appl. Phys. Lett. **66**, 1166 (1995)

SRG with doubled frequency

- **Azopolymer P6a12**
- Film thickness ≈ 1.5 μm
- λ_{rec} = 488 nm, I = 70-750 mW/cm^2
- Polarizations: 0° / 90° (SP), ±45°
- For ±45° polarizations – "normal" frequency of the SRG
- For **0°/90° (SP)** polarizations – **doubled frequency** of the SRG

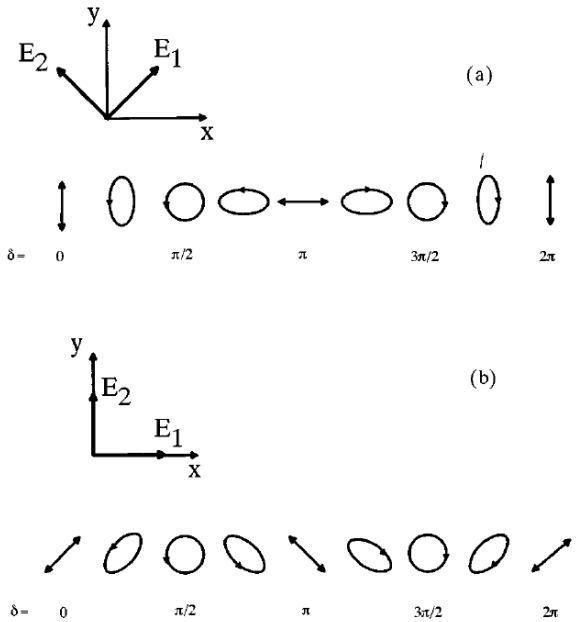

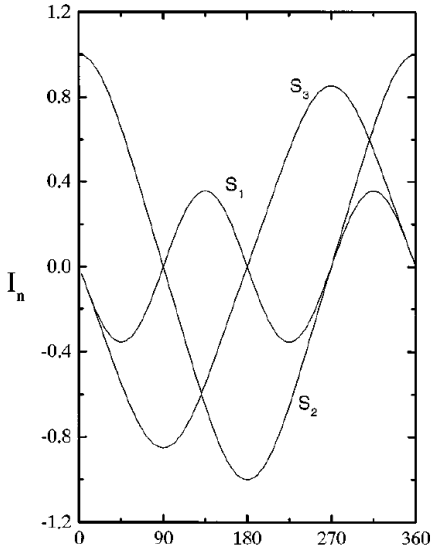

The appearance of doubled frequency SRG is explained with the influence of the waves diffracted in the ±1 orders. They change the polarization pattern **during** the exposure!
(see the $\mathbf{S_1}$ Stokes parameter)

Naydenova et al, J. Opt. Soc. Am. B **15**, 1257 (1998)

Exposure time: 5 s

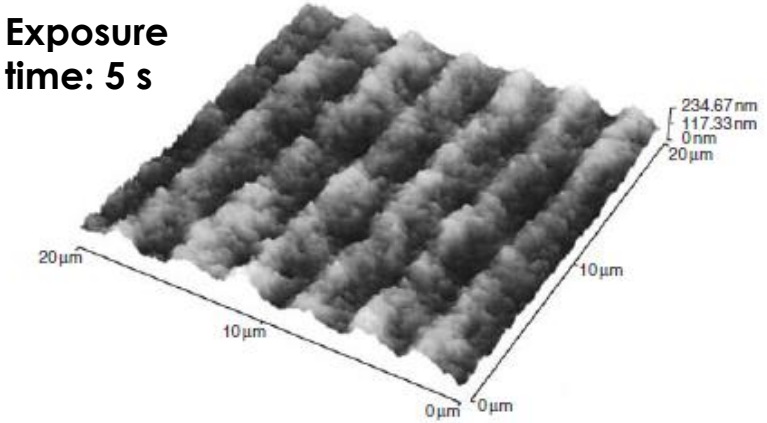

Exposure time: 10 s

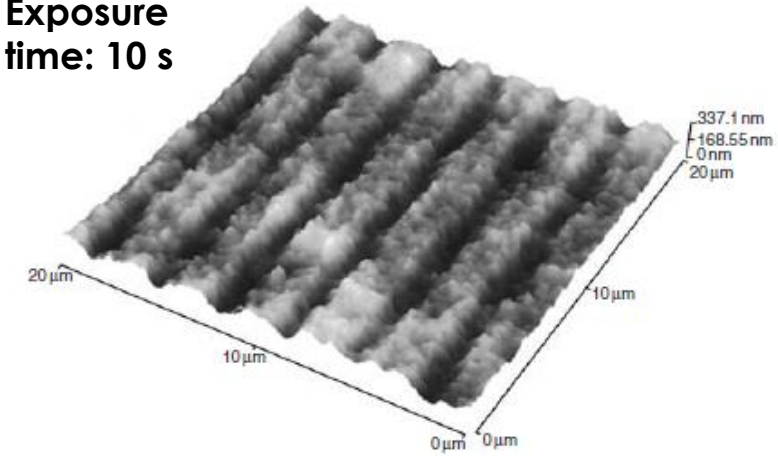

Exposure time: 20 s

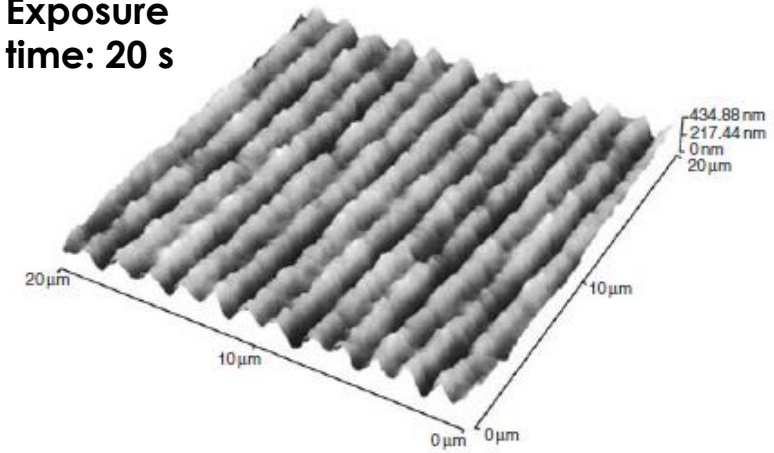

SRG – real time *in-situ* AFM

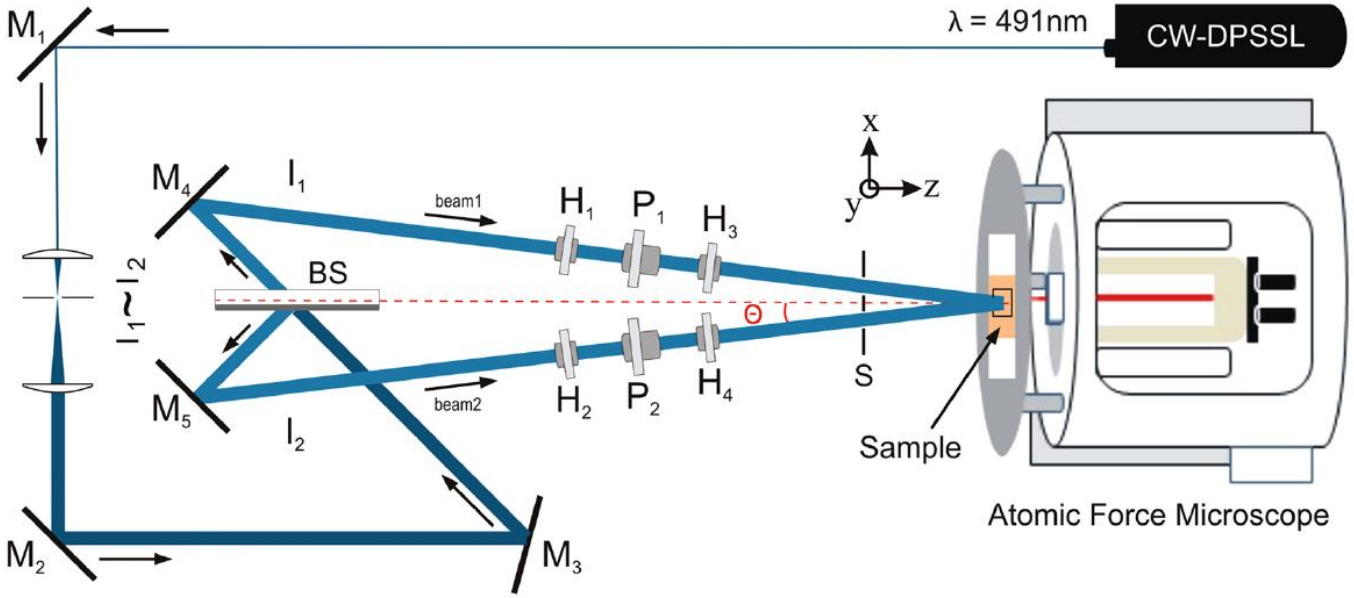

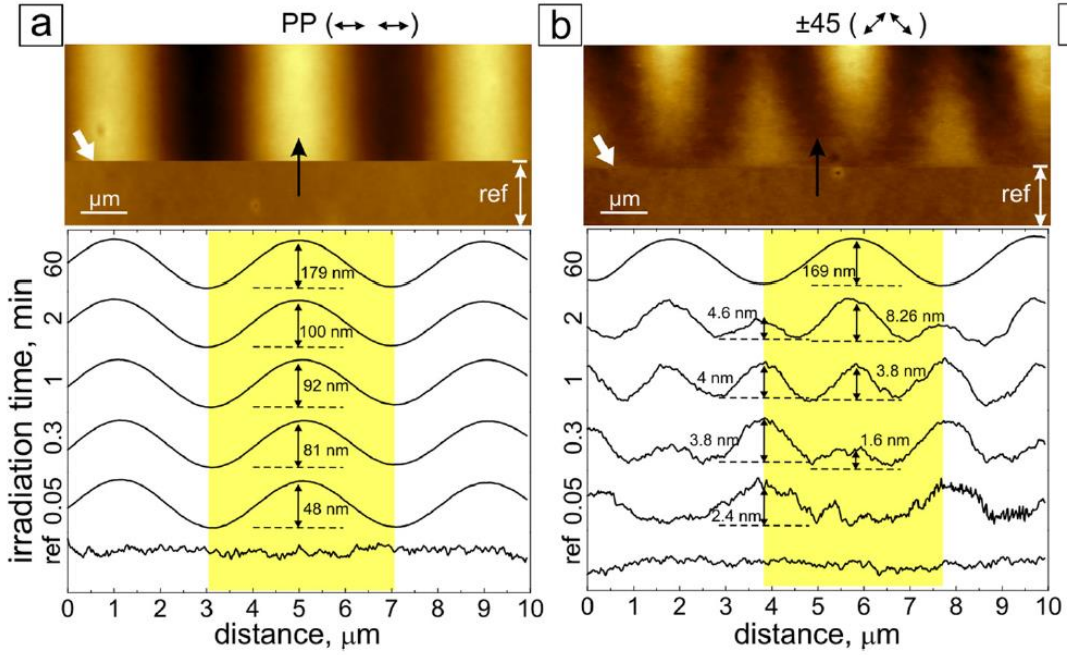

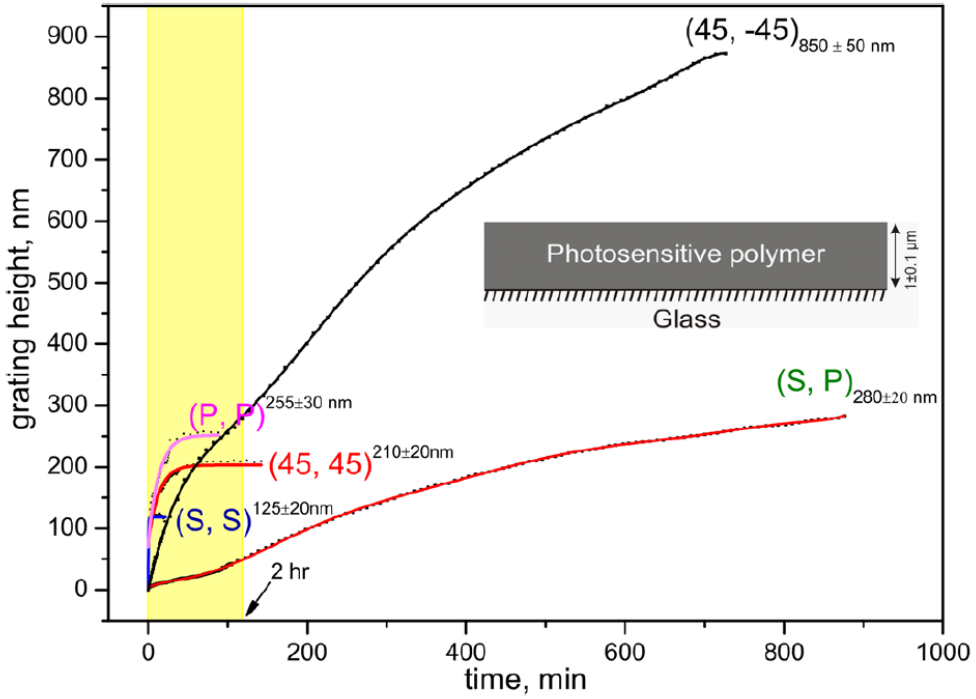

- **Azopolymer PAZO**
- Film thickness ≈ 1 μm
- λ_{rec} = 491 nm, I = 100 mW/cm^2;
- Polarizations: SS, PP, SP, ±45°, RL
- Λ = 4 μm; 9 min scan, 15 x 10 μm
- h_{SRG} = 850 nm (±45°)

Yadavalli et al, J. Appl. Phys. **113**, 224304 (2013)
Jelken et al, Appl. Phys. Lett. **116**, 051601 (2020)

SRG in azopolymers and azopolymer nanocomposites

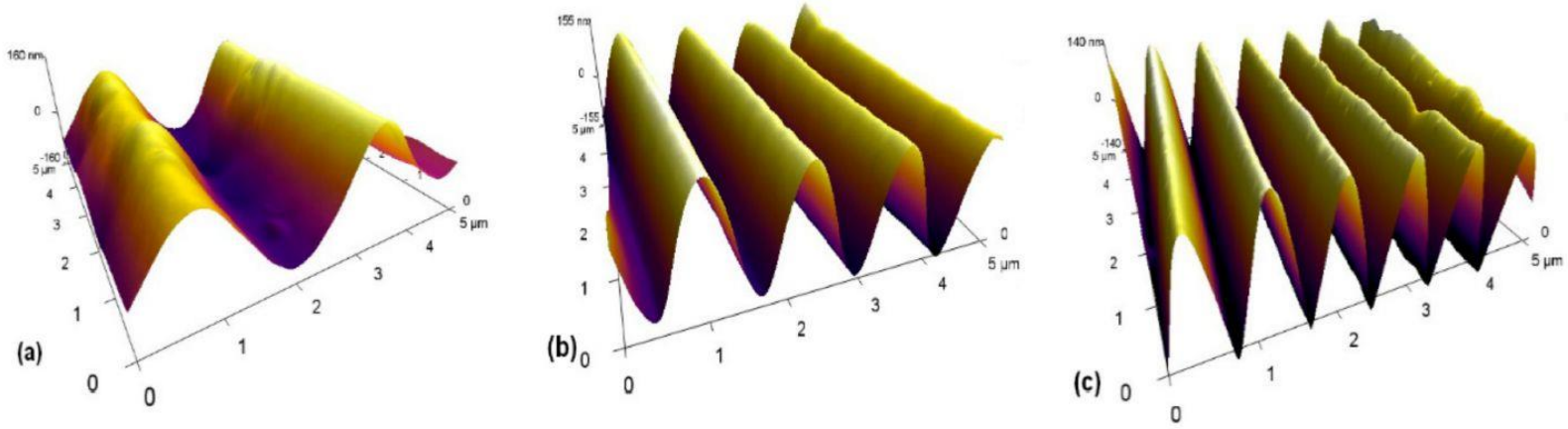

$\Lambda = 2.5\ \mu m$ at $2\theta = 10^\circ$ $\Lambda = 1.3\ \mu m$ at $2\theta = 20^\circ$ $\Lambda = 0.85\ \mu m$ at $2\theta = 30^\circ$

- **Azopolymer PAZO + goethite nanorods**
- Film thickness: 400-470 nm
- λ_{rec} = 442 nm, I = 950 mW/cm^2; L/R CP
- Diffraction efficiency: ***η*** ≈ **53% (+1 & -1 order)**
- Λ = 850 – 2500 nm; h_{SRG}: up to 280 nm

- **Azopolymer PAZO**
- Film thickness: 1800 nm
- λ_{rec} = 442 nm, I = 100 mW/cm^2; L/R CP
- Diffraction efficiency: ***η*** ≈ **35%** (total for all 4 diffraction orders)
- Λ = 1300 nm; h_{SRG} ≈ 160 nm

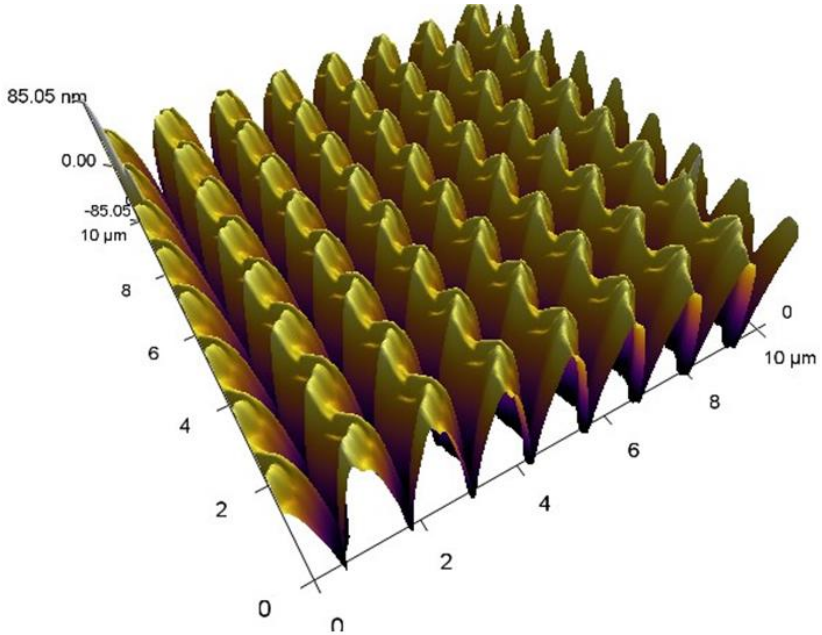

Nedelchev et al, Photonics **8**, 306 (2021)
Mateev et al, J. Phys.: Conf. Ser (2023) in print

Priimagi, Shevchenko, J. Polym. Sci. **52**, 163 (2014)
Oscurato et al, Nanophotonics **7**, 1387 (2018)

Photoalignment of liquid crystals (LC) by azobenzenes

1988

Alignment of LC by photo-oriented ***"command surfaces"*** containing azobenzene.

Advantages:

- Very thin azobenzene films (monolayers or few nm thick) are photo-oriented
- Their orientation is transferred to transparent and highly birefringent media (LC)
- Optically reversible and electrically controllable elements

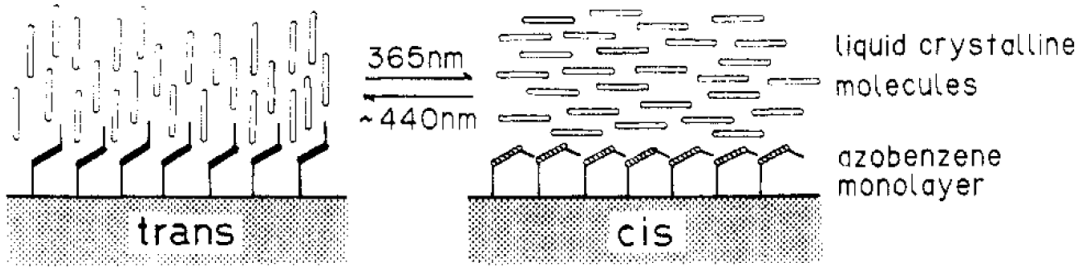

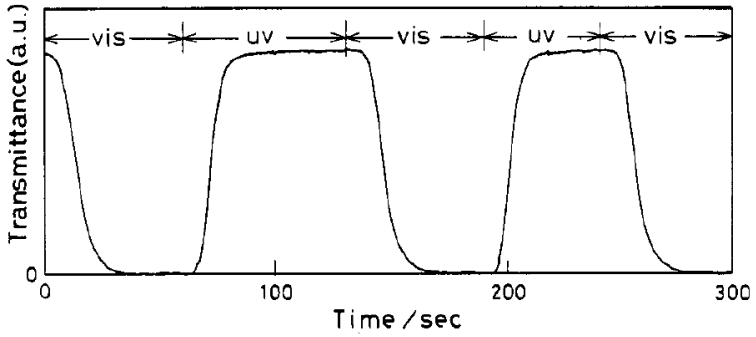

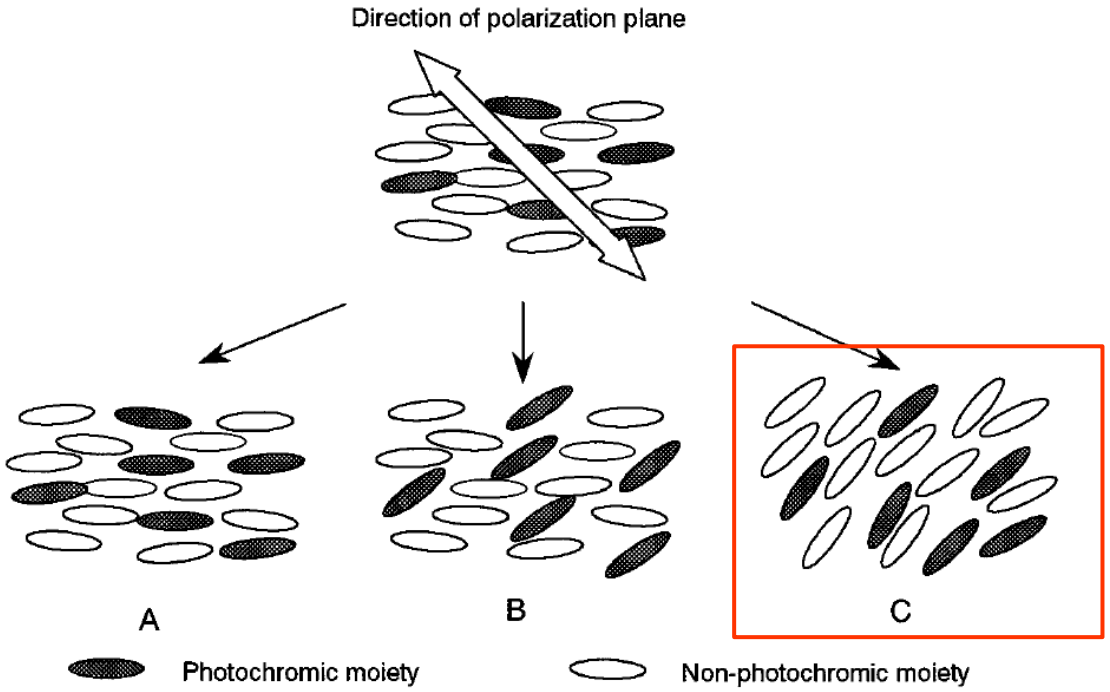

Polymer-dispersed liquid crystals (PDLC)

Ichimura et al, Langmuir **4**, 1214 (1988)
Ichimura, Chem. Rev. **100**, 1847 (2000)
Cipparrone et al, J. Opt. Soc. Am. B **18**, 1821 (2001)

Photoinduced supramolecular chiral structures

(on irradiation with **elliptically** polarized light)

2000

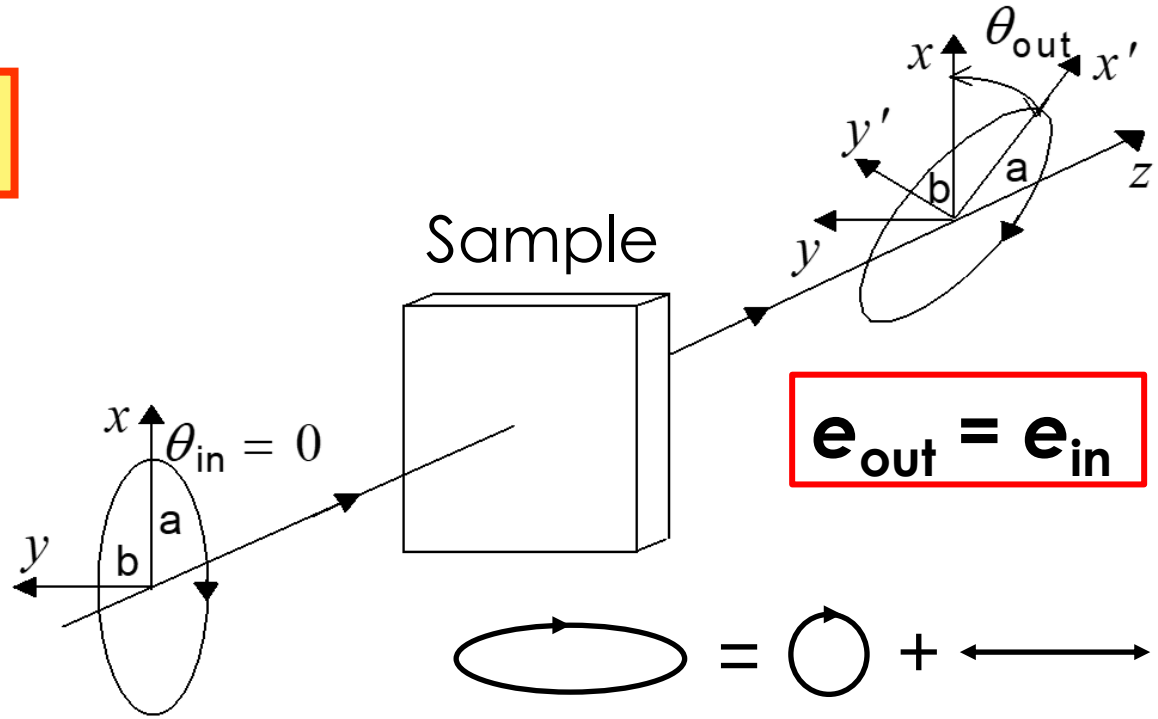

$$e_{out} = e_{in}$$

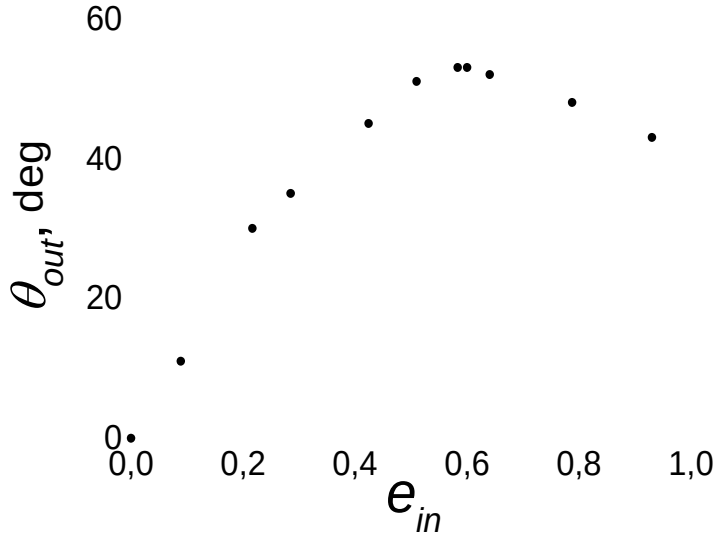

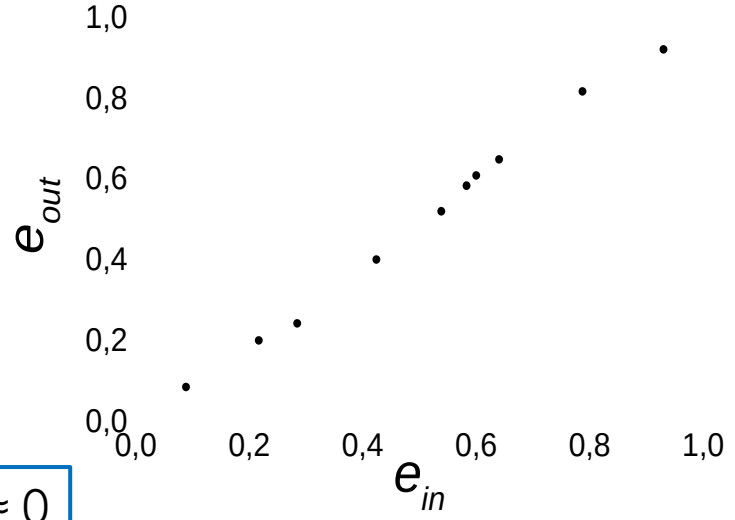

$$\theta(d) = \frac{2e\delta}{1-e^2}d$$

$\boldsymbol{\theta(d)}$ – azimuth rotation
$\boldsymbol{e}$ – ellipticity of light
$\boldsymbol{\delta}$ = πΔn/λ (coefficient)
$\boldsymbol{d}$ - film thickness

$e_{out} = e_{in}$ when $\Delta D \approx 0$

Nikolova et al, Appl. Phys. Lett. **77**, 657 (2000)

Real-time study of chiral structures using polarimeter

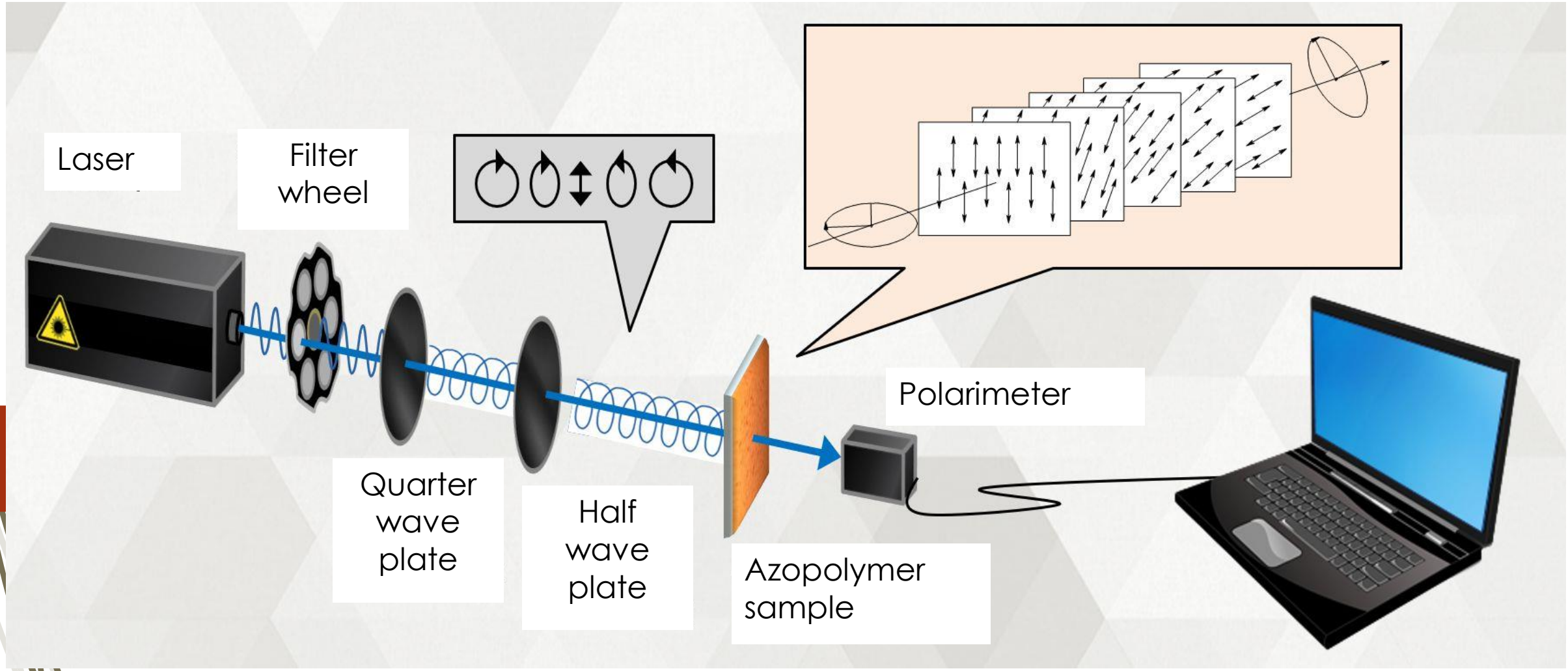

Kinetics of the chiral structures

λ_{rec} = 444 nm

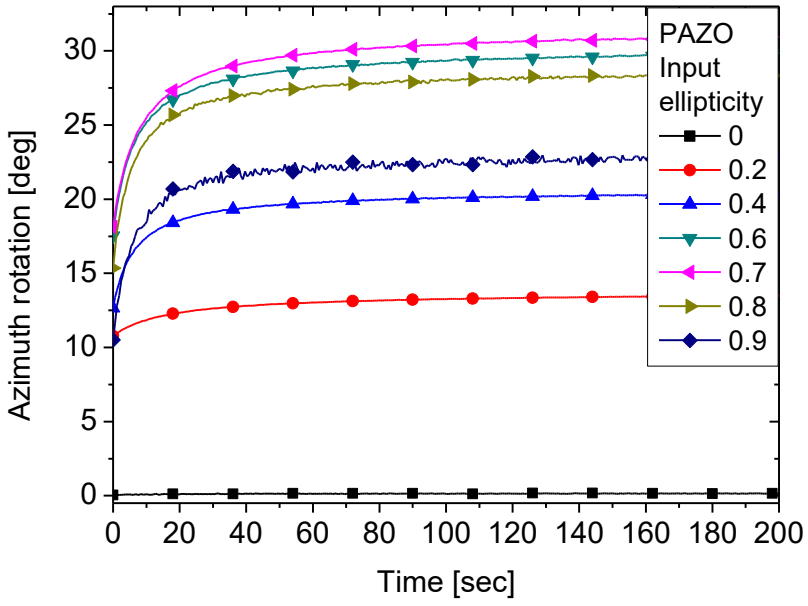

λ_{rec} = 514 nm

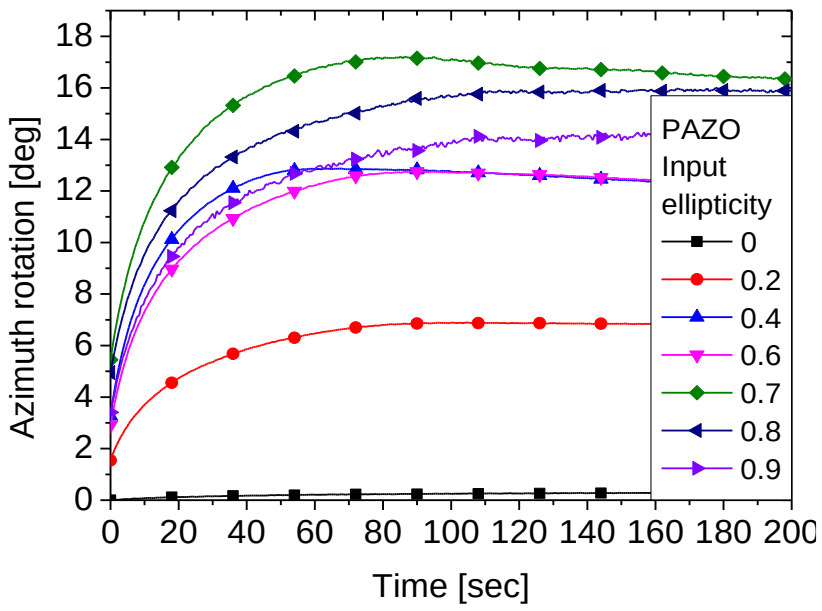

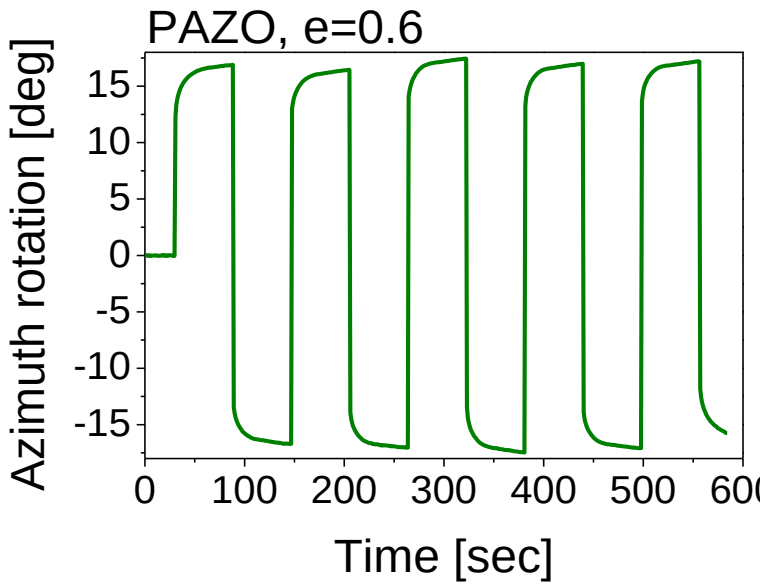

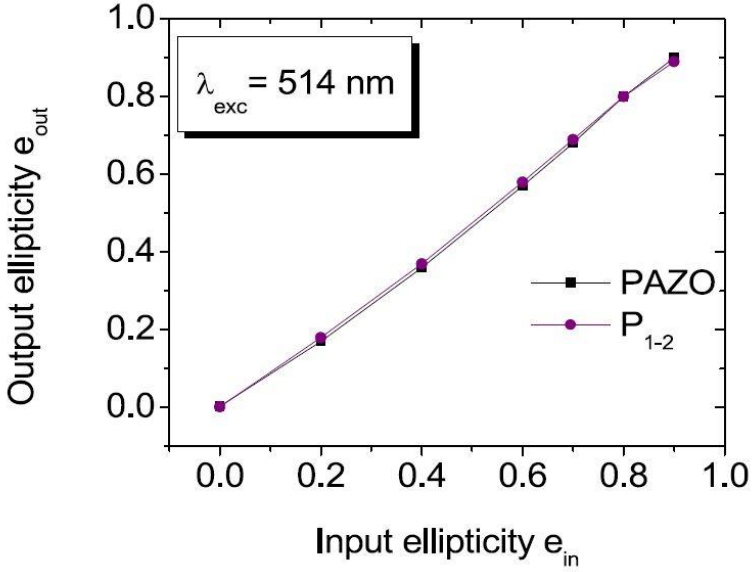

We have studied the influence of the pump beam wavelength and intensity.
The reversibility of the chiral structures has been shown, when the handedness of the input ellipticity is reversed – this indicates possible application in **all-optical switching**.

Blagoeva et al, Appl. Opt **61**, B147 (2022)

Polarization-selective holographic lens

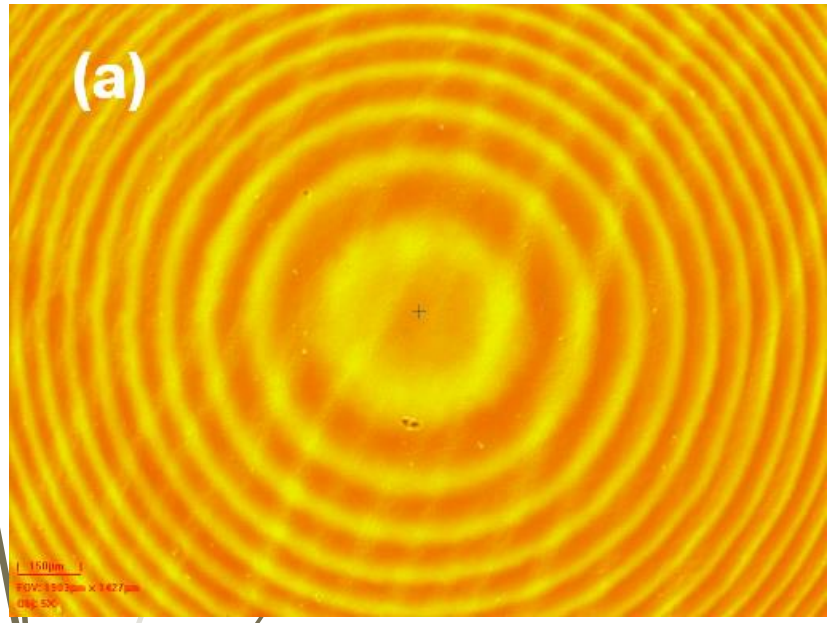

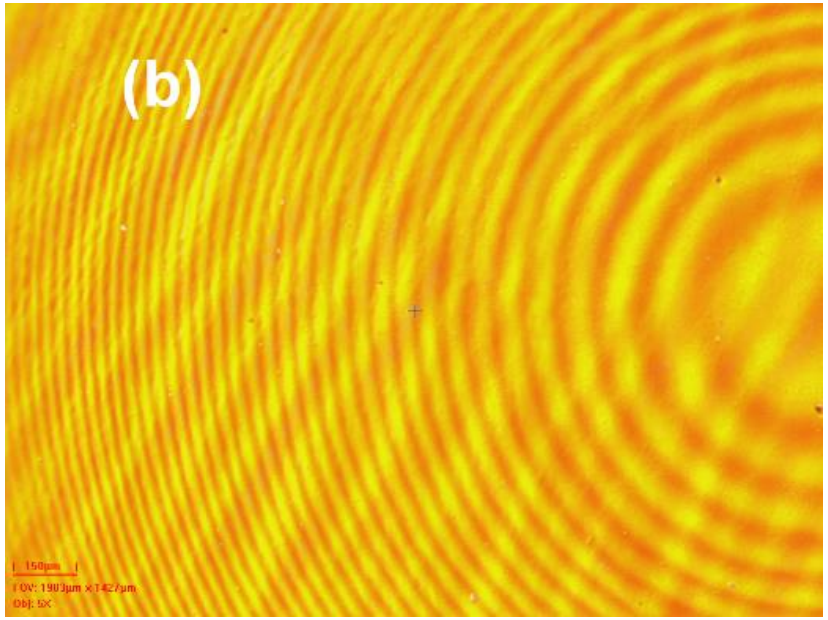

Images of the central part (a) and side part (b) of the lens by polarization optical microscopy

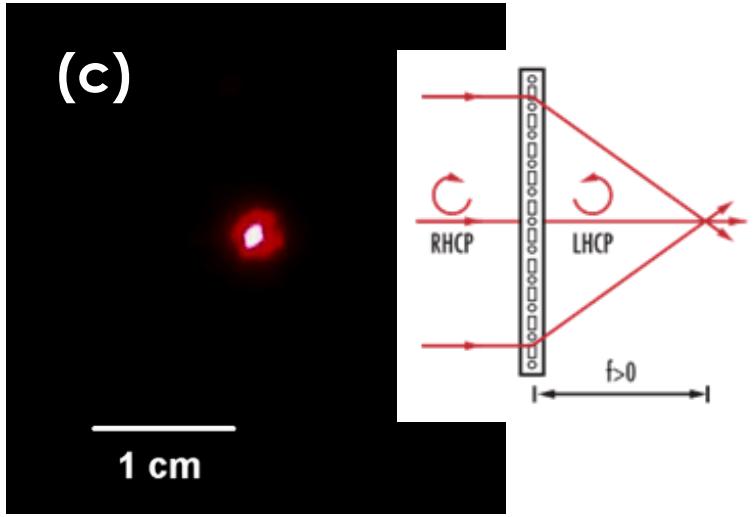

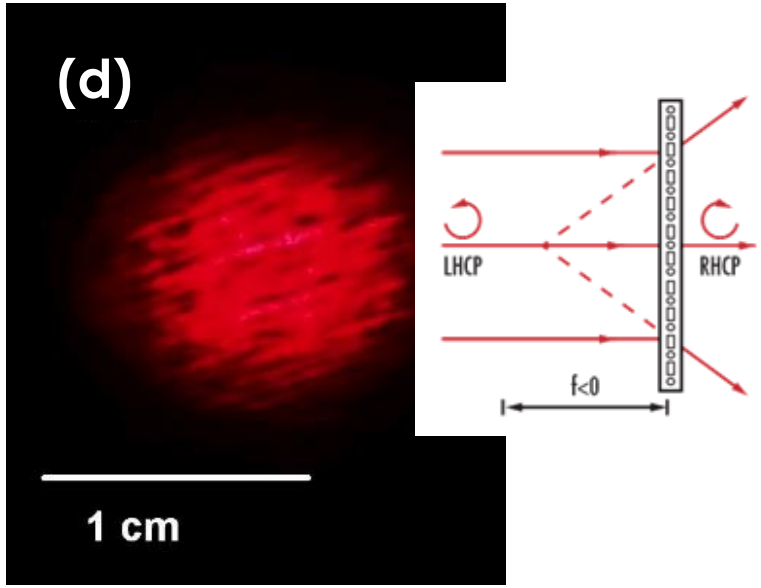

For RCP light the lens is converging(c), but for LCP it is diverging (d).

Nedelchev et al, Appl. Opt. **62**, D1 (2022)
Eich et al, Makromol. Chem. Rapid Commun. **8**, 59 (1987)

Digital polarization holography

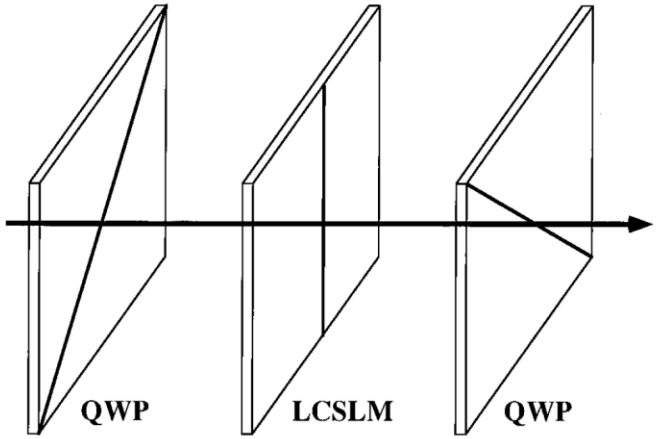

The azimuth rotation angle is **θ = Φ/2**, where Φ is a voltage-dependent phase shift

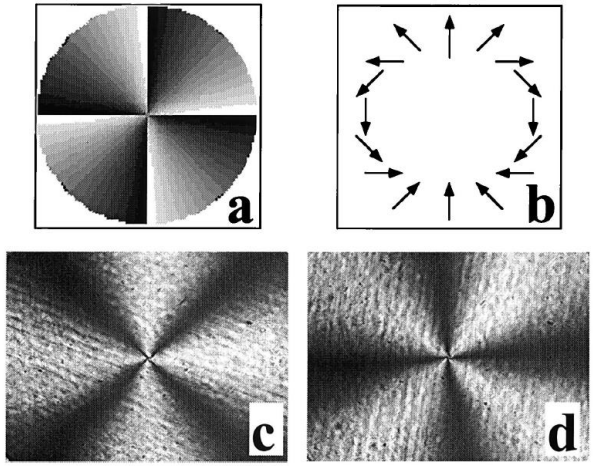

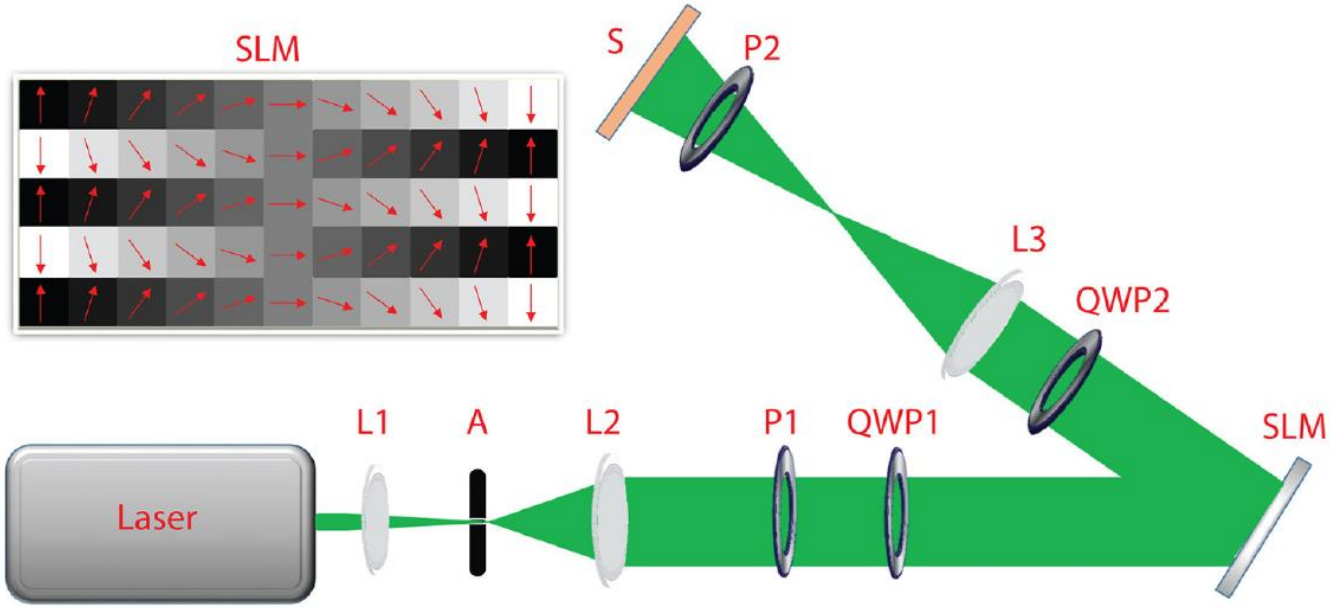

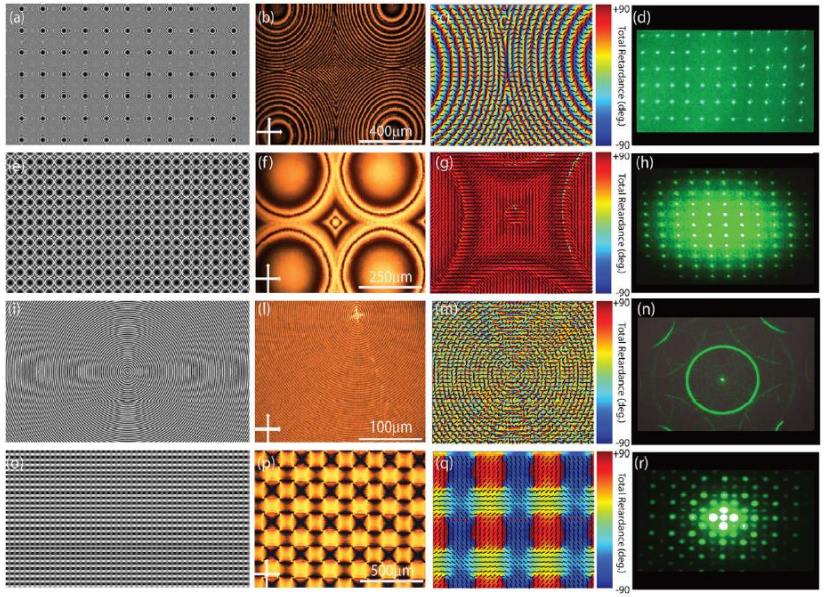

Davis et al, Appl. Opt. **39**, 1549 (2000)
De Sio et al, Opt. Expr. **24**, 18297 (2016)

Acknowledgments

- I am extremely grateful to Prof. Nikolova, Prof. Todorov and Prof. Ramanujam
- Thanks to all my colleagues, who are a constant inspiration
- I'm also grateful for the funding, received through national and international projects

BULGARIAN SCIENCE FUND

ETRI

Inframat

Thank you for your attention!